EIT Waves: A Changing Understanding over a Solar Cycle

M.J. Wills-Davey · G.D.R. Attrill

Abstract We present here a review of observations and the current theories that attempt to explain coronal EIT waves. EIT waves were first observed by SOHO-EIT in 1996. Since then, careful analysis has shown that they are related to various other phenomena, such as: CMEs, coronal dimming regions, Moreton waves, and transverse coronal loop oscillations. Over the years, myriad theories have been proposed to explain EIT waves. Early attempts, while elegant, relied heavily on theories based on pre-coronal observations. More recent work, which tends to consider a larger data pool, has led to two competing theoretical camps: wave vs. non-wave models; in many cases, proposed hypotheses flatly contradict each other. Sifting through these seemingly-incongruous models requires a thorough understanding of the available data, as some observations make certain theories more difficult to justify. However, some questions still do not appear resolvable with current data and will likely require help from the next generation of coronal telescopes.

Abbreviations

AIA	Atmospheric Imaging Assembly;
CME	Coronal Mass Ejection;
EIT	Extreme-ultraviolet Imaging Telescope;
EUV	extreme ultraviolet;
EUVI	Extreme-UltraViolet Imager;
Hα	the Hydrogen Alpha line;
MHD	magnetohydrodynamic;
SDO	Solar Dynamics Observatory;
SOHO	Solar and Heliospheric Observatory;
SECCHI	Sun Earth Connection Coronal and Heliospheric Investigation;
STEREO	Solar TErrestrial RElations Observatory;
SXT	Soft X-ray Telescope;

M.J. Wills-Davey (✉) · G.D.R. Attrill
Smithsonian Astrophysical Observatory, 60 Garden St., Cambridge, MA 02138, USA
e-mail: mwills-davey@cfa.harvard.edu

TRACE   Transition Region and Coronal Explorer;
XRT   X-Ray Telescope.

1 Introduction

Although only discovered a little over a decade ago, "coronal waves"—large-scale, diffuse, single-pulse coronal propagating fronts—have rapidly become part of the heliophysics lexicon. The very first observation of a coronal wave was reported by Dere et al. (1997) during SOHO's first "CME watch" observing program. On 23 December 1996, they observed a coronal wave event at the limb, subsequently associated with a large CME. Shortly thereafter, Thompson et al. (1998) presented the first detailed study of a coronal wave ("EIT Wave"), focusing on the now famous 12 May 1997 event.

While these events have become known colloquially as "EIT waves"—recognizing their initial discovery by the SOHO-EIT instrument (Delaboudinière et al. 1995)—it is important to note that the label "wave" is purely phenomenological; while in many respects they act like waves, several models question this assumption and put forth alternative theories. This review discusses the many observations and various current models that seek to explain coronal EIT waves.

If, in fact, EIT waves are true MHD waves, their detailed observation may offer a unique opportunity to measure otherwise-elusive coronal properties. In such a case, "global coronal seismology" would make it possible to directly quantify local quiet Sun plasma properties (e.g. density, temperature, magnetic field strength). Unfortunately, Warmuth et al. (2005) acknowledges that "probably a considerable fraction of coronal transients [coronal waves] are not really waves at all ... [This] poses a problem for their use as tools for deriving ambient coronal parameters, which require the disturbances to be MHD waves." (e.g. Mann et al. 1999; Ballai and Erdélyi 2004; Ballai et al. 2005; Warmuth et al. 2005; Warmuth and Mann 2005). Before coronal wave behavior can be confidently utilized for global coronal seismology, the physics behind these wave-like phenomena must be clarified.

Part of the reason for the debate regarding the physical nature of EIT waves comes from difficulties in their observation. Until the recent launch of STEREO (Kaiser 2005), EIT waves had generally been observed by the EIT and TRACE (Handy et al. 1999) telescopes. Such observations are problematic for two reasons: (1) the EIT "CME Watch," with its single (195 Å) passband and ∼12–18 minute cadence, limits the number of frames and wavelengths in which these events can be viewed; (2) the limited TRACE field-of-view (8′ × 8′) constrains the viewable range of any passing EIT wave, decreasing the number and extent of recorded events. Such limitations (particularly in the case of EIT) mean that these waves are generally observable in only a few frames, with most of the data showing subtle bright fronts detectable primarily in running difference images. Since the fronts themselves quickly become diffuse—by the later stages, quantitative measures are ineffective, as the waves are virtually impossible to distinguish from noise—observers are constrained to measure the edges of the bright fronts "by eye," often using movies as a guide. Figure 1 (Okamoto et al. 2004) offers one such example.

2 Initial EIT Wave Interpretations

Observations of coronal single-pulse wave phenomena were not wholly unexpected. "Moreton waves", first seen by Moreton (1960) and Moreton and Ramsey (1960), were ob-
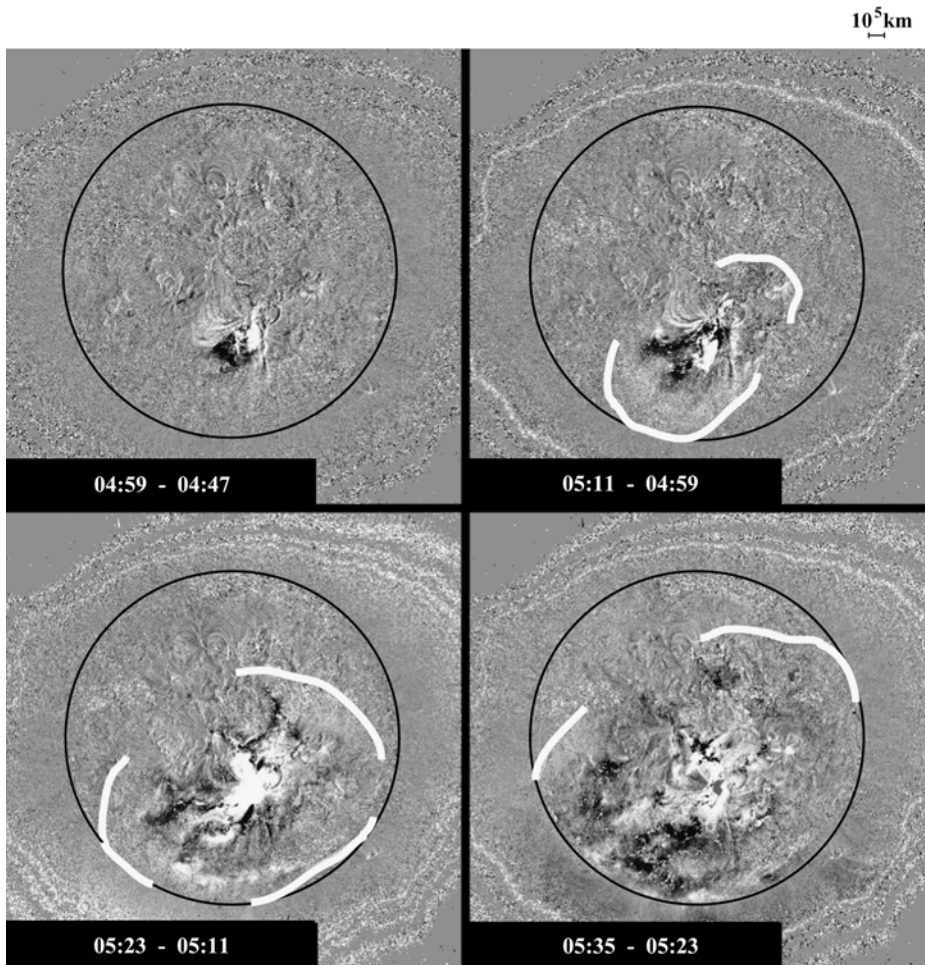
10^5km

Fig. 1 Running difference images of SOHO-EIT 195 Å data from 10 April 2001 (Okamoto et al. 2004). The *black circle* outlines the solar disk, while the *white lines* show the observer's estimation of the wave position, based on visual inspection of the edge of the bright front

served in the Hα 6562 Å line, appearing initially in the ±0.5 red-shifted wing as absorption, and then as emission in the center and blue-shifted wing (Dodson and Hedeman 1968). It is possible to observe this in Hα running difference images as a dark front followed by a bright front (Fig. 2). Moreton waves travel away from flaring regions, and are typically constrained to an arc-shaped propagating front (though not exclusively so—see Warmuth et al. 2005 and Balasubramianiam et al. 2007). They have been particularly noted for their high travel speeds—in some cases, faster than 2000 km/s (Becker 1958; Smith and Harvey 1971).

Based on these data, theories were put forth to explain Moreton waves' predominantly arc- shaped morphology, extremely high velocities, and observed behavior in the ±0.5/0.8 Å wings of the Hα line. As one example, Meyer (1968) suggested they were imprints of trapped fast-mode MHD waves, reflected from the upper corona back down to the chromosphere due to density stratification. However, it was Uchida (1968) who offered
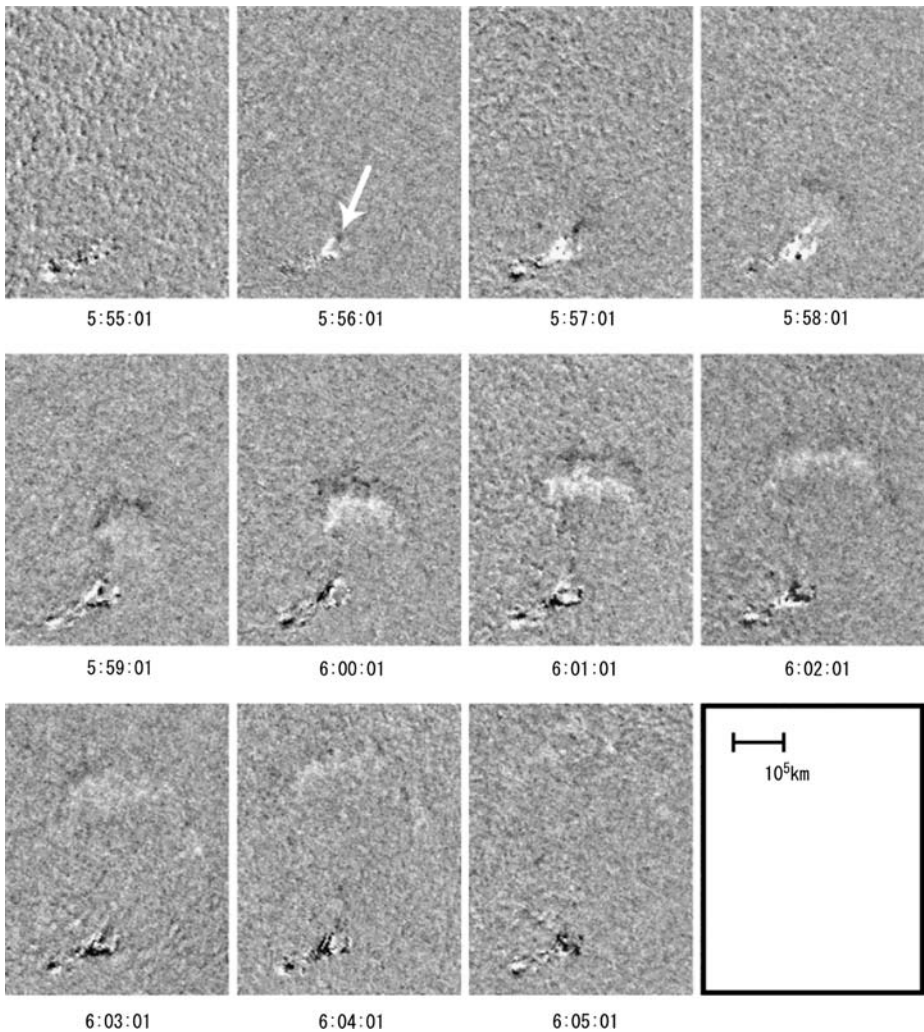
Fig. 2 Running difference images of a Moreton wave observed on 4 November 1997 in the Hα + 0.8 Å wing (Eto et al. 2002)

the most comprehensive rationale. He understood that the appearance of a Moreton wave in the Hα wings could indicate a down-up swing of the chromosphere, and suggested that the chromospheric response was due to compression from a sudden pressure jump in the corona. Thus, Uchida (1968) postulated that Moreton waves must have a coronal counterpart; they were not inherently chromospheric in nature, but rather were coronal fast-mode MHD shock fronts extending down into the chromosphere, producing a "skirt" as the chromosphere was displaced by the flare-induced coronal shock wave (Fig. 3). Unfortunately, the lack of coronal observations at the time made this theory inherently unfalsifiable until the launch of X-ray and EUV imaging spacecraft.

Since EIT-observed phenomena are generally discovered via visual inspection, the earliest EIT wave observations tended to be spectacular events—large, comparatively bright, vir-

Fig. 3 Representation from Uchida ([1968](#)) of an expanding fast-mode coronal MHD shock. *Dashed lines* show the paths of wave packets and *solid lines* show the expansion of the wave front over time
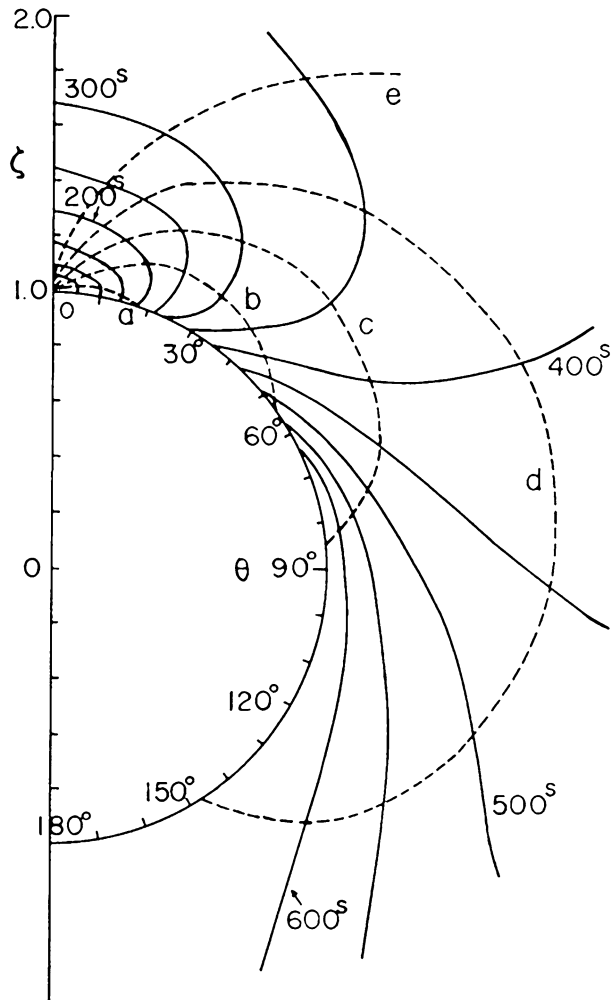
tually circular (often referred to as "semi-isotropic") waves propagating relatively unencumbered from a single active region across a quiet solar disk (e.g. Thompson et al. [1998](#), [1999](#)). At the time, the events themselves seemed remarkably similar: reasonably circular morphology, speeds in a relatively narrow range (200–400 km/s), and lifetimes of ∼45–60 minutes. Additionally, some EUV fronts had associated Moreton waves (e.g. Thompson et al. [2000b](#); Warmuth et al. [2004a](#)). Anecdotally, each of these properties came to be considered as "typical" of EIT waves, and the first postulated theories relied heavily on them.

The average velocity of 200–400 (or, for the sake of argument, 300) km/s drew the most attention. For coronal conditions with small plasma-β ($\beta < 1$), 300 km/s is an entirely reasonable—if slightly slow—fast-mode speed, falling within the expected range of 215–1500 km/s (Wills-Davey [2006](#)). Additionally, fast-mode MHD waves are the only compressional MHD waves able to propagate perpendicularly to the magnetic field. Recalling the long-known, previously unverified Uchida ([1968](#)) work, many concluded that EIT waves were the predicted coronal fast-mode MHD waves (Dere et al. [1997](#); Thompson et al. [1998](#), [2000a](#), [2000b](#); Wills-Davey and Thompson [1999](#); Klassen et al.
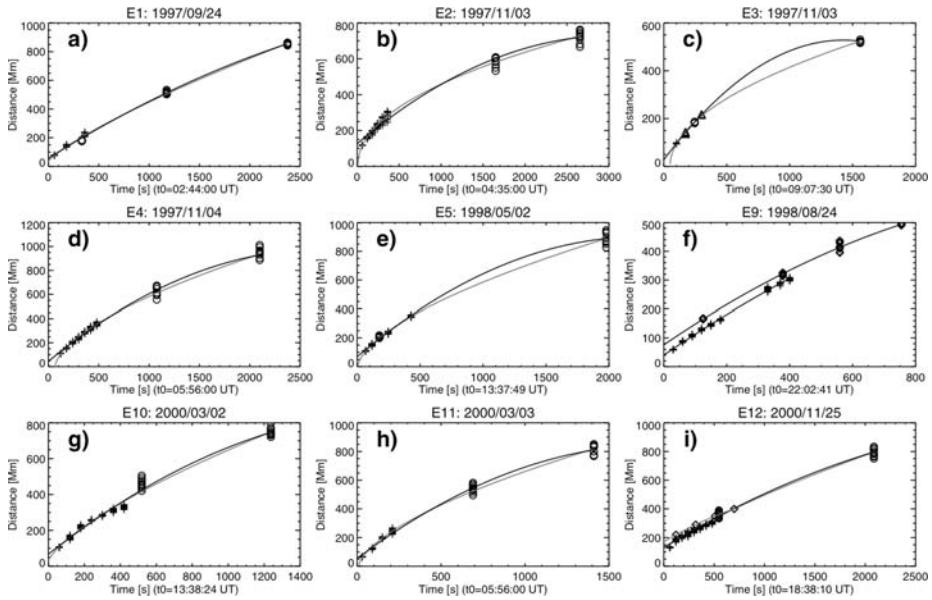
Fig. 4 Results from Warmuth et al. (2004a) showing 2nd degree polynomial (*thick line*) and power-law (*thin line*) fits for combined Moreton wave and EIT wave data. Moreton wave data are shown with *crosses*, and EIT wave data are shown with *circles*

2000; Gopalswamy and Thompson 2000; Vrsnak et al. 2002; Warmuth et al. 2004b; Gilbert and Holzer 2004; Ballai et al. 2005; Vrsnak et al. 2005; Warmuth et al. 2005; Veronig et al. 2006). Several simulations even successfully reproduced known aspects of EUV observations using fast-mode MHD models (Wang 2000; Wu et al. 2001; Ofman and Thompson 2002).

However, unexplained issues still remained. If EIT waves were indeed the postulated coronal counterpart to Moreton waves, why were the two phenomena only rarely observed cospatially?[1] Why was the morphology of most EIT waves (∼93%; Biesecker et al. 2002) broad and diffuse, unlike the sharp, arc-shaped shock fronts observed in the chromosphere? Why were their observed velocities typically a factor of two to three lower than those associated with Moreton waves?

To account for these discrepancies, variations on the Uchida (1968) model were suggested. Warmuth et al. (2001, 2004a, 2004b) postulated that EIT waves really were the coronal counterparts of Moreton waves, provided one accounted for deceleration. Using curved, rather than linear, fits, they were able to account for the motion of several events and resolve the discrepancy between the two wave velocities (Fig. 4).

Alternatively, Chen et al. (2002, 2005) developed a numerical model (Fig. 5) by building on the work of Delannée and Aulanier (1999), who argued that EIT bright fronts were not "waves" at all, but instead plasma compression at stable flux boundaries due to rapid magnetic field expansion. In the Chen et al. (2002, 2005) simulations, a flux rope erupts,

---

[1]It should be noted that the rarity of recent Moreton wave observations over the last few decades makes it difficult to obtain a meaningful sample size for comparison. Note that this is not because of inherently fewer Moreton wave events, but rather that the continuous, high-cadence, full-disk Hα observations required for good Moreton wave coverage are now done with far less frequency than in previous decades.
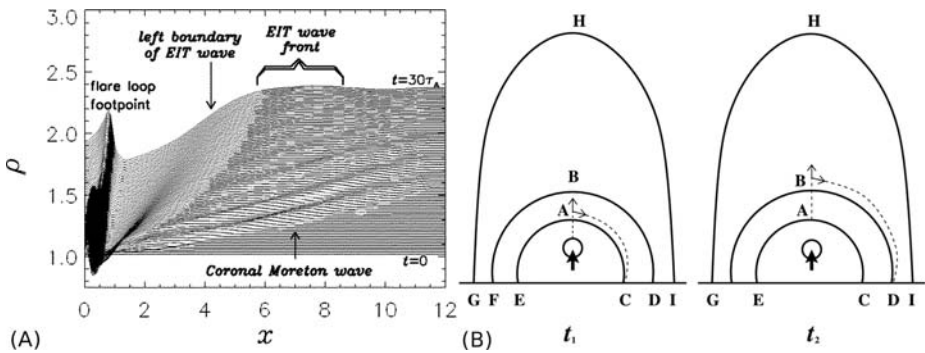
Fig. 5 (**A**) Numerical model of a density distribution due to a Moreton wave and an EIT wave as a function of time (Chen et al. 2002). (**B**) Schematic diagram showing the opening of field lines due to an erupting flux rope. The large-amplitude deformation caused by the erupting flux rope is transferred across the overlying field lines up to point B and along the field line to point C by wave packets. This results in an EIT "wave" bright front generated by successive "opening" of the field lines, producing density enhancements (Chen et al. 2005)

gradually "opening" the overlying magnetic field. The opening-related deformation is trans-
ferred from the top of each overlying field line to its footpoint, successively forming EIT
"wave" bright fronts and creating a propagating density enhancement. Such an eruption
would generate both a Moreton wave—a fast-mode MHD shock, which would quickly prop-
agate away—and a much slower EIT wave—not a true "wave," but rather an expanding
bright front generated as a result of successive density enhancements. Functionally, the EIT
waves in this model could be described as wave-like "wakes" behind Moreton waves; this
not only reproduces their comparatively slow velocities, but also accounts for their broad,
diffuse nature.

The models discussed above, albeit dramatically different wave and non-wave interpre-
tations, offer credible explanations of the aforementioned "typical" EIT wave properties:
they account for ∼300 km/s velocities, they couple EIT waves to Moreton waves, and they
explain the velocity discrepancies between the two phenomena. However, as analysis and
observations have multiplied and improved over time, these "typical" EIT wave attributes
have been found to be less representative than previously thought. In fact, the assumptions
that produced these "typical" attributes can be traced back to two very influential items:
the EIT "CME Watch" cadence, and the study of well-defined events, rather than a more
"representative" sample.[2]

When considered objectively, EIT's ∼12–18 minute "CME Watch" cadence, by its na-
ture, must introduce certain biases. Since EIT waves are identified almost exclusively in
difference images, the lifetime necessary to appear in even one differenced frame is >12–
18 minutes. Additionally, as EIT waves are dynamic, often several frames are necessary to
provide enough data to study; an event must last ∼30 minutes to produce two measurable
frames, ∼45 minutes to produce three measurable frames, and so on. As a result, waves with
lifetimes of >30–45 minutes are likely to be preferentially selected as subjects for study.

---

[2]As, at present, only rudimentary software packages exist that can automatically identify EIT waves (Podlad-
chikova and Berghmans 2005; Wills-Davey 2006), it is important to understand that *all* currently-studied EIT
waves are ultimately viewer-identified. However, some studies (Biesecker et al. 2002; Wills-Davey et al. 2007;
Thompson and Myers 2009) take pains to include less well-defined events, offering a larger range of results.

The requirement of such a long lifetime leads to additional constraints. Only the simplest large-scale dynamic events are likely to remain coherent for >30 minutes as they travel across the solar disk; i.e. circular or semi-circular events tend to be the most easily observed. Additionally, events that propagate at >500 km/s are difficult to observe in multiple "CME Watch" frames; such fast waves are likely to quickly travel over the limb and out of sight, making their on-disk "lifetimes" too short for dynamic study. The result is an artificial upper limit on observable EIT wave speeds.

The second important factor contributing to the "typical" definition of EIT waves is the repeated analysis of a limited number of events, most notably those observed by SOHO-EIT on 12 May 1997 (e.g. Thompson et al. 1998; Wang 2000; Wu et al. 2001; Podladchikova and Berghmans 2005; Attrill et al. 2007a; Delannée et al. 2008) and 7 April 1997 (e.g. Thompson et al. 1999; Wang 2000; Attrill et al. 2007a; Delannée et al. 2008). Both observers and modelers have been drawn to these events for obvious reasons: they are well-defined, display relatively simple morphology (due to their occurrence in the rise phase of solar cycle 23), and are well correlated with other energetic phenomena, such as CMEs and type II radio bursts.

Additionally, the notable interest in the possible connection between EIT waves and Moreton waves resulted in a number of extremely directed studies (e.g. Thompson et al. 2000b; Warmuth et al. 2001; Pohjolainen et al. 2001; Khan and Aurass 2002; Eto et al. 2002; Warmuth et al. 2004a; Okamoto et al. 2004; Temmer et al. 2005; Warmuth et al. 2005; Vrsnak et al. 2005; Veronig et al. 2006; Delannée et al. 2007). While the questions at hand called for examining the few events with definite Moreton wave correlations, the sheer number of these studies led to the erroneous assumption that most EIT waves have associated Moreton waves. While a more extensive database of several hundred events has been compiled (B. Thompson, private communication; Thompson and Myers 2009), only a small number of studies have considered the statistics of large numbers of recorded events (Mann et al. 1999; Klassen et al. 2000; Biesecker et al. 2002; Cliver et al. 2005; Wills-Davey et al. 2007).

The nature of the earliest studies led to unintentional biases both in language and understanding: the large majority of early publications treated EIT waves as fast-mode MHD waves, and they were regularly referred to as "coronal Moreton waves". Such a name implied they were considered to be flare-generated events, given the general consensus at the time regarding the initiation of Moreton waves.

3 Observable Properties of EIT Waves

As time has gone on, and researchers have considered EIT waves—both their properties and their physics—in greater detail, a new, more complex picture has emerged. In part, this is due to additional observations from other EUV and X-ray instruments, such as TRACE, Yohkoh-SXT (Tsuneta et al. 1991), SPIRIT (Zhitnik et al. 2002), GOES/SXI (Lemen et al. 2004), STEREO-EUVI (Wuelser et al. 2004), and Hinode-XRT (Golub et al. 2007). While no other instrument has yet observed as *many* EIT waves as SOHO-EIT, such alternate data sources have provided improved cadence, resolution, and temperature range. Ultimately, the accumulated data have shown that scientists must take a greater variety of characteristics into account when attempting to explain EIT waves.

3.1 Morphology

While many properties of EIT waves now appear to vary greatly from event to event—they are alternatively global, contained; fast, slow; semi-isotropic, complex, etc.—certain

morphological characteristics appear common to all observations. EIT waves are generally found to be a single-pulse phenomenon (a single, expanding bright front). Although homologous events are common, as yet, no observational evidence has been presented showing two consecutive diffuse EIT fronts.[3] In spite of mounting evidence in support of "double" (Neidig 2004; Gilbert et al. 2008) or even "triple" Moreton waves (Narukage et al. 2008), and observations of multiple wave fronts in He I data (Vrsnak et al. 2002; Gilbert and Holzer 2004; Gilbert et al. 2004) associated with EIT wave events, current wavelet analysis of EUV data remains consistent with a single-pulse explanation (Wills-Davey et al. 2007).

Although a small number ($\sim$7%) of EIT observations display sharp, semi-circular wave fronts early in a pulse's lifetime (called "S-waves"; Biesecker et al. 2002 or "brow waves"; Gopalswamy et al. 2000), and limited TRACE observations suggest that even non-"S waves" are well-defined in their earliest stages (Wills-Davey 2006), the data show all EIT waves eventually devolving into broad, diffuse structures, with the bright front widths of the order of 100 Mm. This is not simply an artifact of SOHO-EIT cadence, as evidenced by the higher-cadence TRACE and STEREO-EUVI data (e.g. Wills-Davey 2006; Long et al. 2008). Such increasing diffuseness (Dere et al. 1997; Thompson et al. 1999; Klassen et al. 2000; Podladchikova and Berghmans 2005) is consistent with the amplitude decay of a propagating, semi-isotropic perturbation.

There is also mounting evidence that EIT waves are confined to a region 1–2 scale heights above the chromosphere (confirmed recently by Patsourakos et al. 2009, using stereoscopic analysis). Observations on the solar limb show that most brightenings are observed within several hundred Mm (Thompson et al. 1999; Warmuth et al. 2004a, 2005; Vrsnak et al. 2005). Additionally, analytical calculations by Nye and Thomas (1976) and Wills-Davey (2003) find that changes in Alfvén speed with altitude will result in the "trapping" of laterally-propagating MHD waves below $\sim$2 scale heights. Such findings are consistent with measurements by Wills-Davey (2003), who finds that, as the wave expands, intensity amplitude drops off as r^{-1}, rather than the r^{-2} expected for spherical waves.

The bright fronts themselves are transitory features, with the front increasing the local intensity over a period of a few minutes as the wave passes through. This is true even in high-cadence, emission measure results available for some TRACE events (Wills-Davey 2003). Such transient intensity increases imply some sort of temporary temperature or density enhancement. Unfortunately, as most evidence of such behavior has so far been seen using EUV narrowband filter detectors—such as those on SOHO-EIT, TRACE, and STEREO EUVI—is it difficult to de-convolve temperature and density effects. It should be noted, though, that the observations themselves provide certain constraints. Additionally, there do exist some observations of diffuse coronal waves made by broadband X-ray imagers, namely GOES/SXI and Hinode/XRT (Warmuth et al. 2005; Attrill et al. 2009, see Sect. 3.3).

Considerable evidence exists suggesting that EIT waves increase local density. Warmuth et al. (2005) examine six diffuse bright front events, and see comparable morphology and brightness increases from different filters across a large temperature range (1.5–4 MK); they conclude that only compression could produce such observations. White and Thompson (2005) examine contemporaneous EUV and radio data for an "S-wave" event, and find bright fronts in both. As optically thin thermal free-free emission is only weakly temperature

---

[3]"*Dual* brightenings" have been reported for two EIT wave events by Attrill et al. (2007a), who show that a persistent brightening remains at the outermost edge of the deep, core dimming, while a propagating brightening forms simultaneously at the leading edge of the expanding bright front. In this case, one brightening is stationary, while the other propagates.

dependent ($\propto T^{0.5}$), any increase in radio emission is more likely due to density enhancement. By taking each passband as isothermal (a poor estimate at best), Wills-Davey (2003, 2006) use automated methods to find density enhancements caused by the 13 June 1998 front observed in TRACE data. Since emission measure (*EM*) relates to density (n_e) according to:

$$EM(x) = \int n_e^2 \, dh \tag{1}$$

where (h) is the column depth, it is possible to derive density changes due to the event by using

$$\sqrt{\frac{\Delta EM(x)}{h}} = \Delta n_e \tag{2}$$

Using these methods, Wills-Davey (2003, 2006) show extremely pronounced, *non-linear* density enhancements early in the event's lifetime (>40% above the background). Warmuth et al. (2004b) find EIT observations consistent with this result, recording intensity enhancements of up to 110% above the background. Additionally, Vrsnak et al. (2005) examine a feature in radioheliograph data associated with a Moreton wave and an EIT wave. The radio data were characterized by relatively weak broadband emission, with evidence for optically thin gyrosynchrotron emission. Vrsnak et al. (2005) concluded that the enhanced gyrosynchrotron emissivity could be due to enhanced electron density caused by an MHD fast-mode shock.

While strong evidence for density enhancement exists, other results suggest heating is taking place as well. Wills-Davey and Thompson (1999) observe a front in the TRACE data that appears bright in 195 Å base difference images, but *dark* in the corresponding 171 Å base difference data, implying an intensity *increase* in the hotter passband, but a *decrease* in the cooler one. Since multi-layer EUV channels observe over a relatively narrow temperature range, a "real" intensity change simply shows a change in the amount of observable material near the peak temperature. To account for 195 Å enhancement coupled to 171 Å depletion, Wills-Davey and Thompson (1999) claim that material is heating out of the 171 Å and into the 195 Å passband, consistent with a temperature increase from ∼1 MK to ∼1.4 MK. Gopalswamy and Thompson (2000) report similar observational discrepancies in a multi-passband EIT observation.

The timescales of the subsequent cooling are particularly telling. Under quiet Sun conditions, conductive cooling takes ∼30 minutes, while radiative cooling times extend up to nine hours (Wills-Davey 2003). If either mechanism was at work, heating caused by EIT waves would be visible for much more extended periods of time. This leads Wills-Davey (2003) to suggest that any heating related to EIT wave brightenings may be the result of thermal compression. Ultimately, the various models explaining coronal EIT waves tend to invoke both density increase (plasma compression) and heating.

3.2 Basic Dynamics

EIT waves are generally observed to be dynamic.[4] Even smaller events tend to travel >1 $R_\odot$ through the lower corona (e.g. Thompson and Myers 2009), maintaining their coherence

---

[4]Delannée and Aulanier (1999), Delannée (2000), Delannée et al. (2007) and Attrill et al. (2007a, 2007b) specifically consider *stationary* brightenings, referring to such events as "stationary EIT waves" and "persistent brightenings". While such non-propagating events are certainly EIT wave-related, they may be the result of differing physics. The relevant models are discussed in more detail in Sect. 4.

over global distances. In each case, the bright front broadens and becomes less intense as it travels (e.g. Klassen et al. 2000; Podladchikova and Berghmans 2005); this could be due to energy flux conservation and possibly dispersion. There appears to be no evidence of periodicity as the bright front pulse expands, with wavelet analysis showing the front encompassing a broad range of frequencies (Wills-Davey et al. 2007).

Published studies regarding the dispersion of EIT waves are inconclusive. Warmuth et al. (2004a, 2004b) visually consider eight events in the EIT "CME Watch" data and find evidence of overall pulse width expansion, but do not measure the corresponding full-width at half-max (σ). However, the case study considered by Wills-Davey (2003) using high-cadence (∼75 sec) TRACE data finds that, even though the pulse width increases, σ remains constant at several points along the wave as it propagates, implying no dispersion. Very recent work by Warmuth (A. Warmuth, private communication) uses more quantitative methods, comparing σ as a function of propagation distance across multiple events in SOHO-EIT and STEREO-EUVI data; his results show a trend towards increasing σ over time, implying that dispersion does occur.

To date, EIT waves have only been definitively observed to propagate through the quiet corona (e.g. Thompson et al. 1999; Veronig et al. 2006). They do not travel across active regions (e.g. Wills-Davey and Thompson 1999); they do not penetrate far into coronal holes (e.g. Thompson et al. 1999). Recent observations by STEREO-EUVI appear to show reflection off of a small equatorial coronal hole, with a width approximately that of the incident EIT wave (Gopalswamy et al. 2009).

Determining the evolution of EIT wave velocities has proved difficult, largely due to the broad and ill-defined nature of the diffuse bright fronts. Warmuth et al. (2004a) (Fig. 4) conclude that EIT waves decelerate as they propagate. While their studies focus predominantly on events that include "S-waves", (which, as discussed above, are a small minority and do not appear representative of EIT waves), they also report decelerations for two diffuse bright front events. Other studies, such as Wills-Davey (2003) and White and Thompson (2005), find little or no evidence of deceleration, regardless of "S-wave" morphology. Additionally, a recent case study by Long et al. (2008) (see Sect. 3.4) suggests that existing measurements of EIT wave velocities may have been underestimated as a result of low cadence sampling. Unfortunately, conclusive evidence in this particular debate has been hampered by a lack of necessary data. More and better observations are needed, ideally at high-cadence in the 195 Å passband, where EIT waves are preferentially observed.

In spite of the lack of consensus on velocity evolution, the data clearly show no *typical* EIT wave velocity. The wave fronts exhibit a large range of average speeds (25–438 km/s, for a sample size of 160 events; Wills-Davey et al. 2007) (Fig. 6). In some cases, multiple homologous events show vastly differing speeds (Thompson and Myers 2009). Unless massive global restructuring is taking place with each event, this suggests that the differences are not due to dramatically varying quiet Sun conditions. Wills-Davey et al. (2007) also find a weak positive correlation between velocity and the wave "Quality Rating" (Biesecker et al. 2002; Thompson and Myers 2009), where "Quality Rating" is a subjectively-derived rating of the observer's confidence in the wave measurement (Fig. 6).

Analyses by Podladchikova and Berghmans (2005) and Attrill et al. (2007a) examine well-defined, simple events and find that the bright fronts themselves show evidence of rotation as they expand (Fig. 7). The Attrill et al. (2007a) results from the 7 April 1997 event are particularly compelling; the same ∼22° rotation is observed at two separate positions along the bright front, suggesting a coherent rotation of the entire coronal wave. These observed rotations of the bright front are consistent with the rotations exhibited by associated filament eruptions, as well as with the sense of helicity of the CME source regions (Attrill et al. 2007a).

Fig. 6 Distribution of average EIT wave speeds with respect to "quality rating," a subjective quantity corresponding to the observer's confidence in the measurement (Wills-Davey et al. 2007). This sample of 160 events shows a weak positive correlation. Note the substantial velocity spread
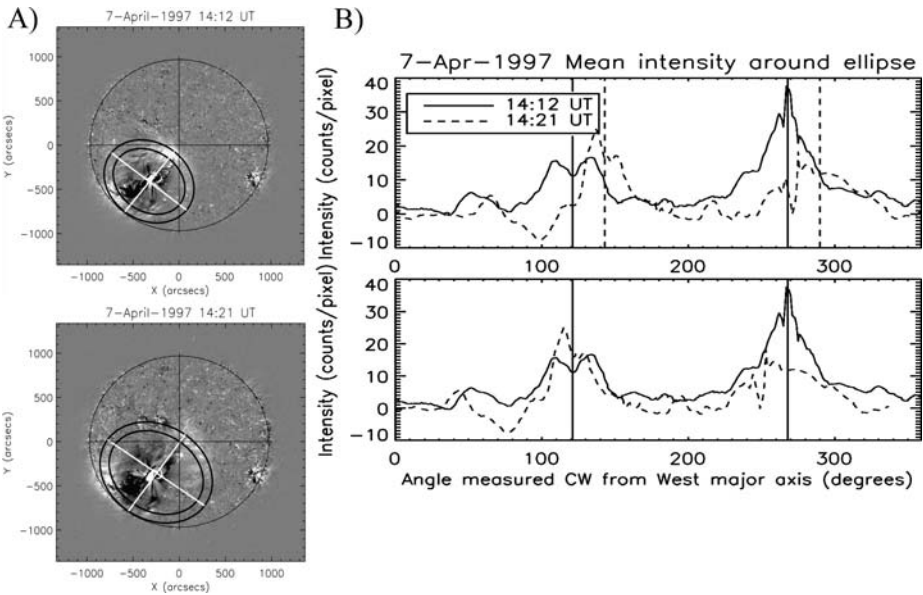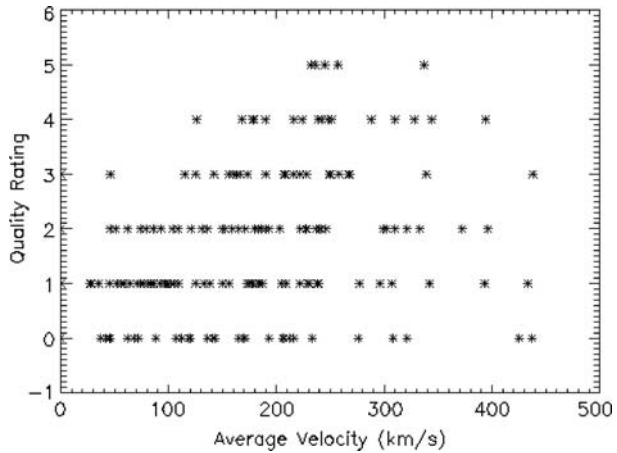

Fig. 7 (**A**) Successive base difference images showing the diffuse EIT wave event of 7 April 1997 (Attrill et al. 2007a). The *bright fronts* are overlaid with concentric *black ellipses*; the *white crosses* mark the axes of the ellipses. (**B**) Quantitative measurements taken from the *black ellipses* in (**A**), showing the mean intensity around the ellipses as a function of the deprojected azimuthal angle. The *vertical lines* mark the weighted mean for each peak. The *upper panel* shows the rotational shift of the mean-weighted peaks. The *lower panel* shows the weighted mean of the later peaks phase-shifted to match those of the earlier peaks

3.3 Observations by Different Instruments

Since EIT waves, by nature, are best observed under full-disk, continuous-viewing conditions, until recently, observations were dominated by the SOHO-EIT "CME Watch" at 195 Å. Except under special circumstances, other EIT-observed EUV wavelengths (notably

171 Å and 284 Å) were only available as part of the daily synoptic (taken typically four times a day), making them generally unsuitable for dynamic wave analysis.

Observations by other instruments have not been as extensive, but they have shown conclusively that EIT waves are detected across the observed EUV range, in addition to 195 Å, including at 171 Å (TRACE; e.g. Wills-Davey and Thompson 1999), 175 Å (SPIRIT; Grechnev et al. 2005), 284 Å (EIT; Zhukov and Auchère 2004), and 304 Å[5] (STEREO-EUVI; e.g. Long et al. 2008). Diffuse global-scale coronal waves have also been observed in soft X-rays by GOES-SXI (Warmuth et al. 2005) and, more recently, by Hinode-XRT (Attrill et al. 2009).

The X-ray results are particularly compelling, as they show that diffuse EIT waves are observable by broadband instruments. Previous observations by Yohkoh-SXT failed to show evidence of diffuse coronal waves; only "S-wave" equivalents were ever observed (e.g. Khan and Hudson 2000; Khan and Aurass 2002; Narukage et al. 2002; Hudson et al. 2003; Narukage et al. 2004; Warmuth et al. 2004a). Similar "S-wave" observations have also been reported in Hinode-XRT data (Asai et al. 2008). For some time, it was thought that this discrepancy was due either to the wave's average temperature—such that diffuse EIT waves would be too cool to observe in Yohkoh-SXT—or to the broadband instruments themselves—with EIT waves being sufficiently diffuse as to be "washed out" in multi-temperature data (Wills-Davey et al. 2007). The recent observations of diffuse, global-scale coronal waves by GOES-SXI and Hinode-XRT suggest that the problem has not been the nature of broadband X-ray telescopes, but rather the improved dynamic range of these newer instruments. Automatic exposure control was heavily implemented during SXT's "flare mode," limiting the dynamic range and impeding observations of the surrounding corona (see the appendices in Hudson et al. 2003 for a full discussion). Additionally, SXT's extensive use of "flare mode" led to the recording of partial-frame, active-region-focused images during the time periods most conducive to global coronal wave production.

Evidence of EIT waves has also been seen in He I data (Vrsnak et al. 2002; Gilbert and Holzer 2004; Gilbert et al. 2004). Vrsnak et al. (2002) report paired wave phenomena, consisting of a main perturbation (described as a diffuse disturbance co-spatial with, but morphologically different from, an Hα Moreton wave) and a forerunner moving ahead of the associated Moreton wave front. Gilbert et al. (2004) examine both chromospheric He I 10830 Å data and coronal Fe XII 195 Å data. They find that the chromospheric and coronal disturbances are cospatial, and interpret the He I signatures not as waves themselves, but rather as chromospheric "imprints" of the coronally-propagating waves. In further analysis, Gilbert and Holzer (2004) also note the occurrence of multiple waves existing in close proximity to each other.

Recent case studies by Long et al. (2008) and Attrill et al. (2009) compare the positions of bright fronts across multiple wavelengths. By degrading the faster cadence of the 171 Å passband and eliminating measurements at 284 Å, Long et al. (2008) measure co-spatial wave position, velocity, and acceleration across 3 wavelengths (Fig. 8).[6] Attrill et al. (2009) analyze a different event, observed by Hinode-XRT as well as STEREO-EUVI, and find that the bright front is largely co-spatial across multiple wavelengths. Surprisingly, their analysis suggests that the front, as observed in hotter passbands, may somewhat *lag behind*

---

[5]We note that the 304 Å He II line contains significant coronal contamination due to 303.32 Å Si XI. This makes it likely that any 304 Å EIT wave observations may still be coronal.

[6]Note that the 171 Å data in Fig. 8 differs between the two panels; Fig. 8 (left) shows 171 Å data until ∼13:07 UT, while Fig. 8 (right) extends those observations out to ∼13:23 UT. This discrepancy is apparently caused by the degradation to a ten-minute cadence (D. Long, private communication).
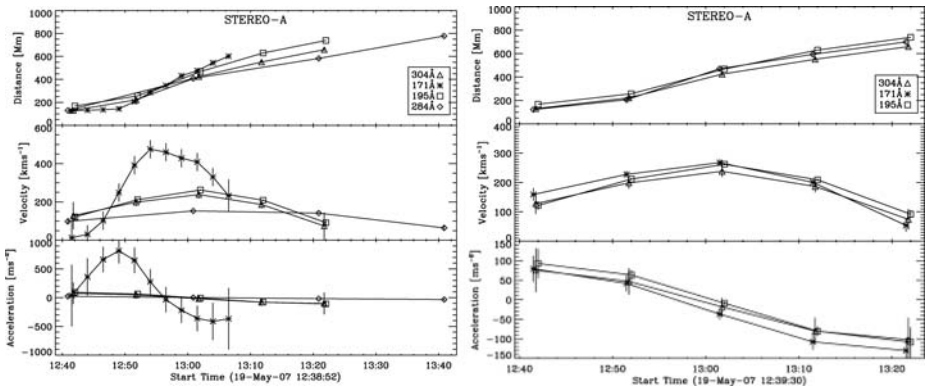
Fig. 8 Plots of distance, velocity, and acceleration of an EIT wave observed on 19 May 2007 (Long et al. 2008). The *left panel* shows the full-cadence STEREO observations, while, in the *right panel*, the data have been smoothed to a 10-minute cadence and the 284 Å data removed. (Note that the 171 Å points are mislabeled in the *right-hand distance plot*. The points are shown as *diamonds*, rather than *stars*.)

the cooler components. However, the diffuse nature of the front makes it difficult to draw any firm conclusions.

3.4 Connection to Other Solar Phenomena

EIT waves do not exist in isolation; they are related to other dynamic events. First and foremost, they have been found to be strongly associated with CMEs, rather than flares (e.g. Moses et al. 1997; Plunkett et al. 1998; Cliver et al. 1999; Biesecker et al. 2002; Okamoto et al. 2004; Cliver et al. 2005; Chen 2006; Attrill et al. 2007a; Veronig et al. 2008; see Vrsnak and Cliver 2008 for a recent review). Coronal dimming regions, understood to be the origins of a significant fraction of the CME mass (Sterling and Hudson 1997; Hudson and Webb 1997; Harrison and Lyons 2000; Wang et al. 2002; Zhukov and Auchère 2004), are always seen at EIT wave origins. Cliver et al. (2005) conclude, from a large statistical study based on the Thompson and Myers (2009) catalogue, that a CME is the necessary condition for EIT wave creation. Attrill et al. (2009) find evidence reinforcing this conclusion, showing that a successful CME is necessary to generate a coronal wave; a failed filament eruption generates neither a bright front nor a CME, while a subsequent successful eruption from the same source, just a few hours later, is associated with both.

In addition, the morphology and kinematics of CMEs appear to influence EIT wave properties. Cliver et al. (2005) show that higher velocity CMEs are more likely to produce EIT waves, suggesting an energetic connection. They also find that EIT waves are associated with wider CMEs, a finding consistent with Yashiro et al. (2004), who note that faster CMEs are wider. Attrill et al. (2007b, 2009) and Cohen et al. (2009) find strong correlations between EIT waves and the flanks of the associated CMEs (see also Fig. 9). Veronig et al. (2008) have recently studied a diffuse coronal wave observed by STEREO-EUVI and concluded that it is driven by the CME expanding flanks. Chen (2009) combines ground-based coronagraph and EIT data to show that the coronal wave bright front is co-spatial with the CME leading loops. Taken together, these analyses present strong evidence for a direct link between coronal waves and CMEs.

Since EIT waves have been shown to be associated with CMEs, it is not surprising that they correlate well with radio bursts. Klassen et al. (2000) find that >90% of Type II radio
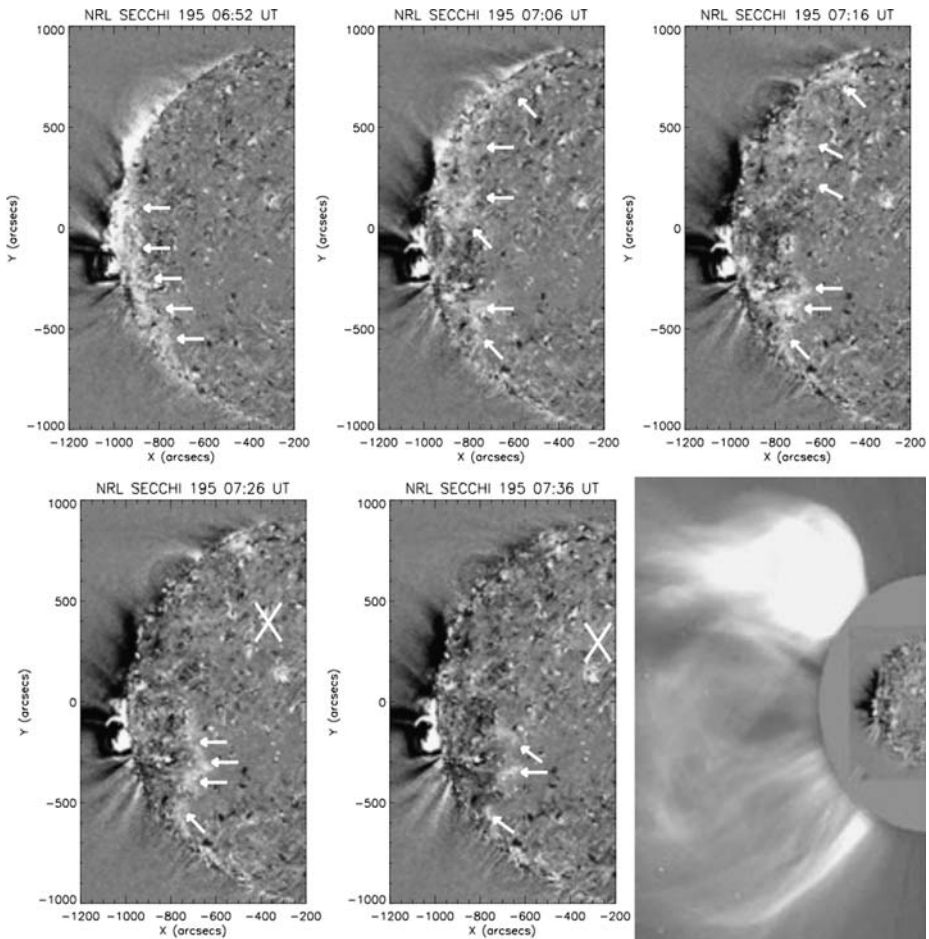
Fig. 9 Base difference images showing a diffuse EIT wave and its associated CME (Attrill et al. 2007b). The bright front is indicated by *arrows*, and diffuse localized brightenings are shown with an "X". The final frame—a composite EUV/coronagraph image (07:36 UT and 07:32 UT respectively)—shows that the spatial extent of the EUV bright front corresponds to the flanks of the CME

bursts have corresponding EIT waves. However, the converse is not true; in their study, Biesecker et al. (2002) find that only 29% of 173 EIT waves are associated with Type II radio bursts. Such a result suggests that coronal shocks are a sufficient, but not necessary, condition for EIT wave production. The correlation is much higher for "S-waves", where all five events seen by Biesecker et al. (2002) have Type II radio bursts. This is consistent with Warmuth et al. (2004b), who find strong correlation between Moreton waves and Type II radio bursts.

While the number of observational examples is somewhat limited (see Footnote 1), numerous studies have pointed out that "S-waves" appear strongly correlated with More-ton waves (e.g. Thompson et al. 2000b; Warmuth et al. 2001; Pohjolainen et al. 2001; Khan and Aurass 2002; Eto et al. 2002; Warmuth et al. 2004a; Okamoto et al. 2004; Temmer et al. 2005; Warmuth et al. 2005; Vrsnak et al. 2005; Veronig et al. 2006; Delannée et al. 2007). However, diffuse EIT waves seem to show poor Moreton wave cor-

respondence, with Biesecker et al. (2002) finding a ~7% association, and Okamoto et al. (2004) a 9% association. Observations also demonstrate a severe velocity discrepancy between the two phenomena, with EIT waves moving at speeds of <450 km/s, and Moreton waves typically traveling >600 km/s. Long et al. (2008) suggest that sampling rate can affect velocity measurements, and suggest that EIT wave velocities may have been generally underestimated (an idea also discussed by Warmuth et al. 2001). However, as velocities found using higher-cadence TRACE data appear in line with EIT measurements (Wills-Davey 2003, 2006), the effects of sampling may require further study.

As EIT waves travel through the corona, they are often observed to deflect magnetic features. EIT wave-instigated filament oscillations have been seen (Okamoto et al. 2004), and numerous observations connect EIT waves to global kink-mode loop oscillations (e.g. Aschwanden et al. 1999; Wills-Davey and Thompson 1999). Interestingly, some loops oscillate, while others appear to be critically damped. Generally, clumps of loops tend to oscillate with nearly the same period, and some observations show that a single source can cause spatially-disparate loop clumps to move with similar periodicity. Terradas and Ofman (2004), Ofman (2005, 2007), and McLaughlin and Ofman (2008) have developed numerical simulations that successfully recreate global kink-mode oscillations. Among other things, these modeling efforts show that overdense loops oscillate preferentially.

4 Theories Explaining EIT Waves

More detailed observations and quantitative analysis have led to multiple theories explaining EIT waves. We review the different interpretations in this section.

4.1 Fast-Mode MHD Waves

The most commonly accepted EIT wave model has been that of a linear fast-mode MHD wave packet (including: Dere et al. 1997; Thompson et al. 1998, 2000b; Wills-Davey and Thompson 1999; Wang 2000; Klassen et al. 2000; Gopalswamy and Thompson 2000; Wu et al. 2001; Ofman and Thompson 2002; Vrsnak et al. 2002; Warmuth et al. 2004b; Gilbert and Holzer 2004; Ballai et al. 2005; Warmuth et al. 2005; Vrsnak et al. 2005; Veronig et al. 2006; Patsourakos et al. 2009; Patsourakos and Vourlidas 2009; Gopalswamy et al. 2009). Uchida (1968) had postulated the existence of a fast-mode coronal counterpart to the chromospheric Moreton wave. When the first EIT waves were observed, they seemed a natural fulfillment of the Uchida (1968) prediction (Dere et al. 1997; Thompson et al. 1999).

While diffuse EIT waves (as opposed to "S-waves", see also Vrsnak 2005) differ from Moreton waves in their dynamics and morphology, much evidence appears consistent with a fast-mode explanation. Any diffuse linear fast-mode MHD pulse should display broadening, such as often observed in EIT waves (Klassen et al. 2000; Podladchikova and Berghmans 2005). Since fast-mode MHD waves—because of their weak dependence on magnetic field direction—are able to propagate perpendicular to the magnetic field, observations should show amplitude drop-offs consistent with blast waves (Wills-Davey 2003). Additionally, shocked large-amplitude wave packets should decelerate to the fast-mode speed (Warmuth et al. 2004a, 2004b).

EIT wave interactions with large-scale coronal features are also consistent with fast-mode behavior. For instance, Uchida (1974) demonstrates that fast-mode MHD waves refract around regions of higher Alfvèn velocity; similarly, EIT waves are observed to refract around active regions (Thompson and Myers 2009). Radio burst observations also fit the

fast-mode MHD explanation, in that even initially slow pulses can steepen into shocks, resulting in Type-II events (Wild and McCready 1950; Nelson and Melrose 1985).

Several numerical simulations have been generated which support the fast-mode wave theory. Using 3D MHD simulations, Wang (2000) and Wu et al. (2001) each successfully model the 12 May 1997 event. Linker et al. (2008) have managed to successfully replicate several aspects of the 12 May 1997 EIT wave observation (such as basic pulse structure and propagation speed) "accidentally," as a by-product of a simulation designed to model CME initiation; they argue that their results are consistent with a fast-mode wave.[7] Numerically-modeled fast-mode solutions have even reproduced related coronal phenomena, including: stationary brightenings (Ofman and Thompson 2002; Terradas and Ofman 2004), global kink-mode loop oscillations (Ofman and Thompson 2002; Ofman 2005, 2007; McLaughlin and Ofman 2008), and the "impenetrability" of coronal hole boundaries (Wang 2000; Wu et al. 2001).

Such a preponderance of evidence might lead to the conclusion that EIT waves are, in fact, Uchida's predicted fast-mode MHD shocks. However, the fast-mode MHD wave explanation also turns out to be inconsistent with numerous aspects of EIT wave observations.

One crucial problem stems from EIT wave velocity measurements. Linear fast-mode MHD waves are constrained to travel within a range of speeds v_{fm}, such that $v_A \leq v_{fm} \leq \sqrt{c_s^2 + v_A^2}$, where v_A is the Alfvén speed and c_s is the sound speed; by definition, their velocities must *equal or exceed* the Alfvén speed. Wills-Davey et al. (2007) address this issue by deriving a range of possible coronal fast-mode velocities (215 km s^{-1} $\leq v_{fm} \leq$ 1500 km s^{-1}), which they compare with EIT wave observations. Of the events considered (Fig. 6), >60% appear to travel below the minimum possible v_{fm}, with speeds that are too slow by as much as an order of magnitude. These discrepancies may simply reflect the findings of Long et al. (2008), who suggest that under-sampling can underestimate "true" EIT wave velocities by up to an order of magnitude. However, a recent reexamination by those authors suggests that under-sampling may have a less pronounced effect than previously thought (J. McAteer, private communication). With this in mind, it appears likely that *some* percentage of the Wills-Davey et al. (2007) events may be traveling below the minimum coronal fast-mode speed.

The recent findings of Zhukov et al. (2009) using high cadence STEREO/EUVI data are even more problematic for the fast-mode wave model. They examine a diffuse coronal wave event, initially traveling at ∼100 km s^{-1}, that undergoes noticeable *velocity changes*—both positive and negative—before accelerating to speeds of ∼200 km s^{-1}. They conclude that such slow speeds and such velocity changes are hard to reconcile a freely propagating fast-mode MHD wave.

In fact, the very *structure of the corona* suggests that $v_{fm} > 200$ km s^{-1} (Wills-Davey et al. 2007). Since the coronal sound speed is roughly 200 km s^{-1}, to treat anything slower as a fast-mode wave requires that the coronal plasma-β must be greater than 1. Under such conditions, gas pressure would dominate magnetic pressure, producing a situation incongruous with coronal observations of well-defined magnetic loops; in effect, the corona would resemble the chromosphere.

Such plasma-β issues are reflected in numerical simulations. In order to successfully model the 12 May 1997 event (mentioned above), Wu et al. (2001) implement extremely high plasma-β's ($5 \leq \beta \leq 50$) over active-region latitudes (see Figure 2 of Wu et al. 2001).

---

[7]It should be noted that the large uncertainties in the Linker et al. (2008) measurements appear to make both a fast-mode and a slow-mode (see Sect. 4.7) explanation consistent with their findings.

Similarly, Wang (2000) accurately models certain aspects of the 12 May 1997 event, but his use of similar quiet Sun parameters for the 7 April 1997 event results in a wave faster than the one observed; interestingly, his 7 April 1997 model shows velocities more consistent with 12 May 1997.

The velocity of a fast-mode/slow-mode MHD wave is typically derived from the following linear solution:

$$v_{f,s} = \frac{1}{2}\left(v_A^2 + c_s^2 \pm \sqrt{v_A^2 + c_s^2 - 2c_s^2 v_A^2 \cos\theta_B}\right) \qquad (3)$$

which depends on the plasma density, magnetic field strength, and magnetic field direction (θ_B). (Slow-mode MHD waves are discussed in Sect. 4.7.) Assuming changes in only the magnetic field direction,[8] the fast-mode speed in the quiet corona will vary by at most 30%. The wave speeds (250–300 km s^{-1}) produced by the Wang (2000) and Wu et al. (2001) simulations reflect this 30% variation.

In contrast, EIT wave observations show much more dramatic variation. Wills-Davey et al. (2007) show that the average velocities of individual EIT waves range over more than an order of magnitude (Fig. 6). For a fast-mode solution to account for event-to-event velocity changes (as mentioned in Sect. 3.2, homologous events traveling at widely different speeds are not uncommon), the global coronal plasma would have to undergo massive, fundamental changes on extremely short timescales (of order a few hours). Interestingly, CME initiation could perhaps account for the necessary level of restructuring.

There is also the question of how to maintain large fast-mode density perturbations over global distances. Extremely large density enhancements ($\sim$40–100%) have been observed during the first few minutes of propagation (Warmuth et al. 2004a; Wills-Davey 2006). With such a rate of steepening, an MHD wave packet will likely steepen, shock, and dissipate, except in very specialized conditions (see Sect. 4.7). If observed pulse broadenings are the result of shock dissipation, the breakdowns would be periodic—in effect, showing "ripples." The analysis of this issue so far is inconclusive, with Ballai et al. (2005) and Wills-Davey et al. (2007) using the same results to draw very different conclusions.

4.1.1 "S-Waves" and Moreton Waves as Fast-Mode MHD Waves

It should be noted that any inconsistencies with a linear fast-mode MHD model apply specifically to *diffuse* EIT waves. The original Uchida (1968) model appears to account very well for "S-waves" and their corresponding Moreton waves (see Sect. 3.4). In fact, dynamic evidence of coronal shock fronts, contemporaneous with Moreton wave observations, has been found in both EUV (Neupert 1989) and soft X-ray data (Khan and Hudson 2000; Khan and Aurass 2002; Narukage et al. 2002, 2004).

The morphology of soft X-ray waves (see Sect. 3.3) differs dramatically from that of global diffuse EIT waves.[9] The soft X-ray data show a front much like the well-defined edge of a "dome" or "bubble," which can be linked to the associated Moreton wave (Narukage et al. 2004; Fig. 10); this is consistent with the 3D expansion of a shock front. Narukage et al. (2004) derive the fast-mode Mach number (M) of the front, and find that, consistent

---

[8]Typically, quiet Sun magnetic field strength or density variations occur on scales of, at most, a few Mm. Given the substantial cross-section of EIT waves, it is unlikely that such small variations will materially influence propagation; only larger-scale differences should be perceptible. Observational analysis (e.g. Wills-Davey 2006) appears to support this.

[9]This description does not include the global XRT event recently studied by Attrill et al. (2009).
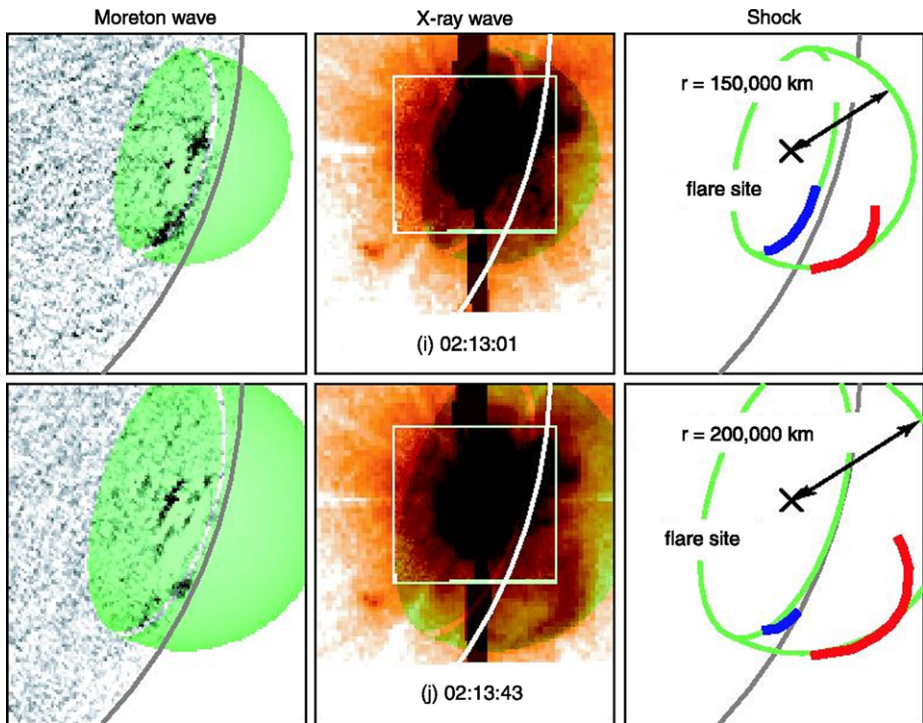
Fig. 10 (Color online) Cartoon of the 3D structure of an MHD shock wave, derived from observations (Narukage et al. 2004). The *left panels* show running difference images of the Moreton wave, the *center panels* show the soft X-ray wave (*negative color table*), and the *right panels* outline wave front observations in the context of the 3D shock structure (Moreton wave: *blue*, soft X-ray wave: *red*)

with shock behavior, it decreases as it propagates. They also find that the Moreton wave *disappears* at $M = 1$—strong evidence that the Uchida (1968) theory is correct.

Comparisons of EUV "S-waves" and Moreton waves (Thompson et al. 2000b; Warmuth et al. 2004a, 2004b; Warmuth 2007) show rough cospatiality, findings consistent with "S-waves" as the EUV components of corona shock fronts. However, as Fig. 4 demonstrates, the EUV data are still insufficient to draw firm conclusions. In the Warmuth et al. (2004a, 2004b) studies, deceleration curves are derived primarily from Moreton wave data. However, because of the slower cadence, each event includes only one or two EUV wave observations. While Fig. 4 shows clearly shows Moreton wave deceleration, the EUV data are inconclusive; constant velocity fits might work equally well (and in some cases, better) for the EIT wave events. Additionally, in assuming *constant* deceleration, Warmuth et al. (2004a) show some events slowing to unphysical speeds (see Sect. 4.1), making the findings more problematic. Unfortunately, until good higher-cadence EUV data are available, the connection between "S-waves" and Moreton waves must rely on consistency rather than conclusion. It is worth noting that recent studies of diffuse coronal waves using STEREO/EUVI data have shown evidence for constant velocity rather than deceleration (e.g. Kienreich et al. 2009; Ma et al. 2009).

4.2 "Wakes" of Moreton Waves

The "wake" theory developed by Chen et al. (2002, 2005) for understanding EIT waves differs in many respects from the fast-mode explanation; however, justification for both interpretations come from many of the same observations. In cases where "S-waves" and Moreton waves are observed co-spatially, later frames always show a diffuse EIT wave rather than an "S-wave" (e.g. Thompson et al. 2000b; Biesecker et al. 2002; Warmuth et al. 2004a). These observations suggest several possible explanations. It may be that "S-waves" devolve and become diffuse, and that the lack of any observations of this transition is due to the slow cadence of current EUV imagers.

On the other hand, the Chen et al. (2002, 2005) model treats Moreton waves ("S-waves") and EIT waves as separate (but related) phenomena. They assume the diffuse bright front is generated during an eruption by the "opening" of overlying magnetic field (see Sect. 2). The Chen et al. (2002, 2005) model interprets Moreton waves as components of coronal fast-mode MHD shock fronts, and requires that EIT waves travel behind these fronts at lower speeds. At present, more robust observations are required to validate this model, since no contemporaneous Moreton wave/EIT wave event has yet been observed by higher-cadence EUV instruments.

Because the Chen et al. (2002, 2005) model is two-dimensional, certain aspects are difficult to test. For instance, the EIT "wave" disruption relies on the displacement of overarching field, and specifically requires the presence of a giant overlying arcade. This suggests that such overarching structures must permeate the quiet Sun corona through which the EIT wave travels. Unfortunately, the lack of such large interconnected structures in quiet Sun limb observations appears to contradict this supposition, making it difficult to explain how this model can produce and sustain semi-isotropic diffuse coronal waves.

The Chen et al. (2002, 2005) model has proved difficult to reconcile with the lack of Moreton waves observed in conjunction with EIT wave events; observations have shown that more than 90% of EIT waves lack an associated Moreton wave (Biesecker et al. 2002; Okamoto et al. 2004). Additionally, these Moreton waves are expected to have longer lifetimes and propagate farther than EIT waves. Some observations do lend themselves to these results; studies have shown evidence of "winking filaments," possibly caused by weakened, and therefore undetectable, Moreton waves (Smith and Harvey 1971; Eto et al. 2002). Such observations suggest not a lack of coronal shock fronts, but rather a lack of *observable* coronal shock fronts (P.F. Chen, private communication); in effect, such shock fronts may be produced as part of every EIT wave event, but are, for all intents and purposes, undetectable.

The observational analysis of Harra and Sterling (2003) is often cited as support for the Chen et al. (2002, 2005) model. Their visual analysis of the TRACE-observed 13 June 1998 event concludes that two related fronts can be seen, with a weak component "dispers[ing] out of the bright wave." In contrast, other observational studies (Wills-Davey and Thompson 1999; Delannée 2000) interpret the same data as possessing only a single moving front. Using automated detection methods, Wills-Davey (2006) also finds evidence of only a single propagating compression front. Before supporting or discounting any of these results, however, it is important to address the assumptions inherent in each study. While the Harra and Sterling (2003) findings are largely qualitative, they do consider the extent to which the Chen et al. (2002, 2005) model may be consistent with their analysis. In contrast, the other studies (particularly Wills-Davey and Thompson 1999 and Wills-Davey 2006) inherently assume only a single compression front, negating any possible validation of the Chen et al. (2002, 2005) model. Wills-Davey (2006) does address the limitations of her automated methods—noting the visual existence of dynamics unaccounted for in her tracking.

It is clear that analysis must be performed in such a way as to make the Chen et al. (2002, 2005) model falsifiable. A step in this direction, has already been undertaken by Cohen et al. (2009). Their global MHD simulation strives to match observations of the CME without making assumptions about specific physical mechanisms responsible for generating the coronal wave signature. To an extent, the findings of Cohen et al. (2009) support the basic physics of the Chen et al. (2002, 2005) model, though a wave front with the high velocities typical of Moreton waves is not found in their work. Most recently, Chen (2009) presents a limb case study demonstrating the spatial correspondence between an EIT wave and the leading loops of the associated CME.

4.3 Stationary Brightenings

Many EIT wave observations show associated stationary coronal brightenings—areas persistently bright in EUV that appear to be instigated by the EIT wave moving through the region. These brightenings are often, but not always, found to occur along pre-exisiting magnetic separatrices (Delannée and Aulanier 1999; Delannée 2000; Delannée et al. 2007; Attrill et al. 2007a, 2007b). Different explanations of these brightenings have been offered, each consistent with the data. The earliest study showed the stationary brightenings to be located at magnetic separatrices. More recently, Delannée et al. (2007) assume a non-wave model and demonstrate that such brightenings may be caused by joule heating arising from the dissipation of current sheets. Attrill et al. (2007a, 2007b) and Cohen et al. (2009) associate such persistent brightenings with the sites of ongoing magnetic reconnection events. Conversely, an MHD wave or shock is capable of triggering a localized energy release when it crosses pre-existing coronal structures. Ofman and Thompson (2002) and Terradas and Ofman (2004) are able to simulate stationary brightenings (specifically at the footpoints of loops), since the energy release causes localized heating and a stationary emission enhancement. The fact that stationary brightenings can be explained by such disparate models suggests that, while they must fit into a cohesive EIT wave model, they are not a likely constraint.

4.4 Successive Magnetic Reconnections Driven by the Flanks of CMEs

Attrill et al. (2007a, 2007b) propose that the diffuse EIT "wave" actually corresponds to the outermost flanks of the CME as it expands in the low corona, with the bright front itself the result of magnetic reconnections between the outermost shell of the CME and favorably-oriented surrounding magnetic field. The coronal "wave" will naturally stop when the internal pressure is no longer large enough to drive the reconnections (van Driel-Gesztelyi et al. 2008, see Attrill 2008 for a detailed discussion). Compelling observational evidence is offered for the EIT wave-CME flank connection (Attrill et al. 2007b; Mandrini et al. 2007; Veronig et al. 2008; Attrill et al. 2009; Cohen et al. 2009; also see Fig. 9). Such an understanding is consistent with Moore et al. (2007), who find that the final angular width of a CME depends on the pressure balance and energy flux conservation between the erupting bubble and the surrounding magnetic field. In contrast, recent work by Delannée (2009), in analyzing a pre-event potential field extrapolation of the 12 May 1997 event, concludes that the two associated dimming regions are straddled by permanently *closed* magnetic field structures, preventing the expanding CME field lines from reconnecting with the surrounding quiet Sun. However, this conclusion contradicts the many studies that connect coronal dimmings to greatly expanded ("open") magnetic field associated with outflowing plasma—hence the terminology "transient coronal holes" (e.g. Rust 1983; Webb et al. 2000;
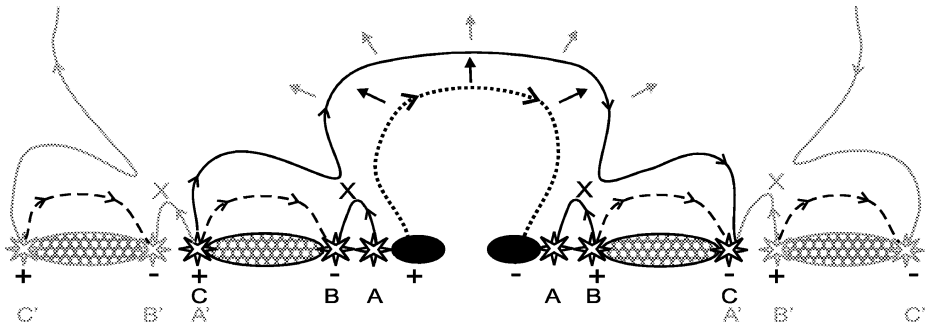
Fig. 11 Cartoon illustrating the Attrill et al. (2007a) model of successive magnetic reconnections. The expanding CME (*dotted line*) reconnects (*crosses*) with favourably orientated magnetic loops (*dashed lines*), causing the magnetic footprint of the CME to expand (*solid line*). "Strong" core dimmings, corresponding to flux rope footpoints, are shown in *black*, while secondary "weak" dimmings are shown in *hatched gray*

Harra and Sterling 2001; Mandrini et al. 2005; Attrill et al. 2006, 2008; Harra et al. 2007; Imada et al. 2007; McIntosh et al. 2007).

Wen et al. (2006) report observations of Type-IV non-thermal radio bursts at the locations of diffuse coronal wave bright fronts, which they interpret as signatures of CME-associated coronal reconnection. Attrill et al. (2007a, 2007b) argue that the concept of reconnections between the expanding CME and surrounding magnetic field is consistent with the Wen et al. (2006) interpretation. In addition to the "strong" core dimmings associated with CME flux rope footpoints (Sterling and Hudson 1997; Webb et al. 2000; Mandrini et al. 2005; Crooker and Webb 2006; Attrill et al. 2006), they also observe widespread, secondary ("weak") dimmings (Thompson et al. 2000a) appearing behind the bright front as it expands. Attrill et al. (2007a, 2007b) explain such observations as the opening of surrounding quiet Sun magnetic fields via successive reconnections, and subsequent plasma evacuation (Fig. 11). Several studies find that observed EIT wave morphologies (as well as the corresponding secondary dimmings) are consistent with the expected reconnection between a laterally-expanding CME and a magnetically-favorable environment (Attrill et al. 2007b; Mandrini et al. 2007; Cohen et al. 2009). Since this concept requires that both secondary and core dimmings are the result of plasma evacuation, spectroscopic quiet Sun measurements will act as an important validation.

The magnetic connection between the diffuse coronal "wave" and the erupting CME can also account for observations of coherent bright front rotation (Podladchikova and Berghmans 2005; Attrill et al. 2007a). Given the eruption source region and the surrounding magnetic environment, the Attrill et al. (2007a, 2007b) model predicts where the bright front is expected to persist, based on the orientation of the surrounding magnetic field; it also predicts the expected locations of secondary dimmings. These aspects give information on the CME source regions and on the magnetic connectivity of the ICME to the Sun.

Certain aspects of models and observations cannot be accounted for with the Attrill et al. (2007a, 2007b) model. For example, the Linker et al. (2008) "accidental" EIT wave simulation produces a coronal wave under reconnectionless conditions. Further study is needed to help resolve such issues. Indeed, the recent results of Cohen et al. (2009) global MHD simulation of a recent STEREO/EUVI event shows that both wave and non-wave components (including magnetic reconnection) are likely required to produce all observed characteristics of EIT waves.

4.5 Bright Fronts due to Electric Currents

Delannée and Aulanier (1999) and Delannée (2000) first proposed that EIT waves are the result of large-scale coronal restructuring due to the CME. More recently, Delannée et al. (2008) use a 3D MHD model, described in Török and Kliem (2003), to show that large-scale, narrow, and intense current sheets form at the beginning of the dynamic phase of the CME. These current sheets naturally separate the twisted flux tube from the surrounding potential fields. The Delannée et al. (2008) simulations show how an almost spherical current shell should form around the expanding CME. Such a model is consistent with on-disk observations of nearly-circular events, and is additionally capable of explaining the rotation observed in some EIT wave events.

However, this electric current model is not entirely consistent with observations. The physics of the heating mechanism itself turns out to be problematic (see Sect. 3.1). Current heating should cool via conduction. However, conductive cooling times in the quiet Sun corona are ∼30 minutes. If EIT wave-affected areas underwent conductive cooling, evidence of the bright front's passage would remain over the length of the cooling time; as a result, EIT waves would appear as bright *disks*, rather than single-pulse bright fronts.

Although successful at reproducing on-disk coronal wave fronts, this mechanism cannot account for limb observations (e.g. Attrill et al. 2007b), since the requirement for line-of-sight integration over the altitude of the current shell is not met. Delannée et al. (2008) state that "EIT and SXT waves are coronal structures (i.e. they evolve at quite high altitude)," and argue that "the dissipation of…current densities at low altitude would not be responsible" for the EIT wave. However, observations show that these wave fronts brighten plasma primarily within the lowest 1–2 scale heights (Patsourakos et al. 2009). While this could simply be the effect of scale height density drop-off, the Delannée et al. (2008) current shell model also requires that the bright front initially *accelerate* as it propagates. In contrast, reported velocity changes vary dramatically from event-to-event, showing deceleration (e.g. Warmuth et al. 2004a; Long et al. 2008), constant velocity (e.g. Kienreich et al. 2009; Ma et al. 2009) or acceleration half an hour into an event (e.g. Zhukov et al. 2009).

4.6 Slow-Mode MHD Waves

Krasnoselskikh and Podladchikova (2007) and Wang et al. (2009) consider the possibility that, rather than fast-modes, EIT waves may be slow-mode MHD waves. Such a postulation is supported by two strong pieces of observational evidence: (1) most EIT waves travel at velocities unphysically slow for coronal fast-modes (Wills-Davey et al. 2007; Fig. 6), and (2) slow-mode wave morphology is more consistent with the non-linear density perturbations observed in EUV. This second piece of evidence is easily demonstrated by simulating even the simplest MHD conditions (i.e. Wills-Davey and Sechler 2007). Assuming a uniform, non-perpendicular magnetic field, the creation of a single one-dimensional MHD perturbation must result in both a fast-mode and a slow-mode pulse traveling away from the initiation point. As it propagates, the density component of the slow-mode pulse rapidly increases to several times that of the initial perturbation, such that an initially linear pulse can become non-linear. In contrast, the fast-mode pulse is dominated by the magnetic field component, with a density component that drops to a fraction of the initial perturbation. When considered in the context of the non-linear intensity enhancements recorded by Warmuth et al. (2004a) and Wills-Davey (2003, 2006), the idea of a slow-mode component appears much more plausible.

In spite of such evidence, other aspects of a slow-mode MHD wave model are problematic. The most compelling may be the requirement of parallel or oblique fields to sustain a

slow-mode wave packet. Equation (3) shows that the slow-mode velocity approaches zero as the magnetic field becomes perpendicular. Wills-Davey et al. (2007) address this problem by arguing that the structure of the closed-field quiet Sun corona likely possesses sufficient horizontal field to sustain a sufficiently large slow-mode wave packet. Since EIT waves are broad, diffuse structures, they will encounter the closed-field quiet Sun as an *ensemble field*, rather than perceiving small, individual loop structures; under such conditions, it is unlikely that an EIT wave should run into sufficient perpendicular field to impede its progress. Notable exceptions are the boundaries of coronal holes, where the perpendicular, open field will act as a barrier. Interestingly, EIT waves are, in fact, observed to "stop" at the edges of coronal holes (e.g. Thompson et al. 1999).

Even if sufficient horizontal fields exist in the quiet corona to sustain a slow-mode solution, other issues must be dealt with. While most EIT waves are too slow to be fast-modes, by the same token, many such waves are too fast to be slow-modes. Slow-mode waves are constrained to the velocity range $0 \leq v_s \leq c_s$; with a quiet Sun coronal sound speed c_s of ∼180 km/s, so a large percentage of events cannot be accounted for (Fig. 6). Additionally, many of the problems inherent in a fast-mode wave model—the difficulties in maintaining pulse coherence, the inability to account for front rotation on a global-scale—are equally hard to account for with a slow-mode model.

4.7 Solitary Waves

While aspects of the slow-mode MHD wave model present problems (for the reasons presented in Sect. 4.6), some of these issues can be dealt with by constraining the form of the MHD wave itself. Wills-Davey et al. (2007) argue that, while a generic non-linear MHD wave packet cannot account for observations, a *solitary* (or soliton-like) MHD wave can.

Solitary waves are, by definition, non-linear, single-pulse solutions to the wave equation. However, instead of steepening and shocking, the shape of a solitary wave is maintained by a balance between the pulse's nonlinearity and the dispersive nature of the medium. The result is a nonlinear, dispersionless wave packet capable of traveling great distance. Additionally, solitary wave velocities depend on *both* the local medium and the pulse amplitude. Therefore, different waves should travel different speeds, with "larger" waves traveling faster.

Many of the expected properties of solitary waves appear consistent with observations. Studies show evidence of nonlinear density and intensity enhancements (Wills-Davey 2003, 2006; Warmuth et al. 2004a). Using the Thompson and Myers (2009) "Quality Rating" as a rough proxy for pulse amplitude, Wills-Davey et al. (2007) find a positive correlation between "Quality Rating" and average EIT wave speed (Fig. 6). Additionally, Wills-Davey (2003) fails to show dispersion for the TRACE-observed 13 June 1998 event, although more recent work appears to contradict this finding (A. Warmuth, private communication).

If EIT waves are assumed to specifically be slow-mode MHD solitary waves, the dispersion-nonlinearity balance and the velocity-amplitude dependence makes it possible to extend the range of likely velocity observations beyond the slow-mode shock speed of c_s, accounting for the entire velocity range of EIT wave observations.

Although the solitary slow-mode MHD wave solution has many powerful components, like all freely propagating MHD wave theories, it cannot explain the coherent rotational aspect of EIT waves (Podladchikova and Berghmans 2005; Attrill et al. 2007a). Since a very specific shape is required to maintain stability, the solitary MHD wave model is also difficult to test and prove. Wills-Davey et al. (2007) argue that the most likely reason for dispersion is the coronal density stratification. While many MHD solitary wave solutions exist, dispersion is usually considered only along the boundary of a flux tube, and as yet,

no work has been done incorporating gravitational density stratification. Additionally, analytical solutions typically address 1D MHD solitons, and work addressing 2D radial propagation is elusive. There is also the fact that quantitative studies find a great deal of structure in EIT wave cross-sections (Podladchikova and Berghmans 2005; Wills-Davey 2006; Attrill et al. 2007a). This implies that any solitary wave solution must be extremely stable, in order to maintain coherence as it affects different components of the quiet Sun corona.

5 Next Steps and Future Directions

To move forward with our understanding, it is vital that any model describing EIT waves be fully consistent with the observations. To do this properly, we need to move away from observer-selected events, which tend to be brighter and better-defined. Consistent, representative samples (for instance, recording every front-side EIT wave) must be gathered. This will likely require automated quantitative tracking, such as the NEMO software package (Podladchikova and Berghmans 2005) or the automated methods of Wills-Davey (2006). Ideally, such tracking algorithms will do more than just record EIT wave kinematics. They should also find other metadata (e.g. density enhancement; Wills-Davey 2006).

At present, automated methods are still difficult to apply. SOHO-EIT ultimately suffers from signal-to-noise problems and has a relatively low cadence. TRACE has sufficiently high spatiotemporal resolution, but an insufficient field-of-view. STEREO-EUVI offers high-cadence, full-disk observations in the 171 Å passband, but generally only a 5–20 minute cadence in the hotter passbands; this is especially problematic for quantifying 195 Å data, where the bright fronts are preferentially observed. Additionally, as STEREO moves farther from Earth, the quality of these data will only decrease, due to lower telemetry rates. Signal-to-noise issues can be compensated for using increased exposure times; however, overly-long exposures could smear dynamic wave front observations, resulting in less precise measurements; the trade-offs of these competing techniques need to be more fully considered.

New observations are necessary to enable us to comprehend the full picture of EIT wave formation and evolution. For instance, the elusive Moreton wave-EIT wave transition has never been captured. Successful observation of this event (if, indeed, it exists) will do much to constrain EIT wave models. At the very least, full-disk, high-cadence, continuous EUV data are required to move beyond our current understanding. As EIT waves originate from CME- (and by association), flare-producing regions, improved dynamic range is paramount. Higher cadence data are also needed to better understand dynamics close to the EIT wave origin. Additionally, to perform meaningful quantitative analysis, it is also necessary to obtain these data across multiple passbands (or, ideally, in multiple spectral lines, as produced by an imaging spectrograph).

The Atmospheric Imaging Assembly (AIA; Title 2006), to be launched aboard the Solar Dynamics Observatory (SDO; Schwer et al. 2002) in 2010, should fulfill some of these requirements. A full-disk imager with ∼0.5″ pixels, SDO-AIA will capture the EUV corona in seven passbands every 10 seconds. It remains to be seen if the photon efficiency of SDO-AIA is sufficient to record events as subtle as diffuse EIT waves. There is also the fact that SDO will be launching near solar minimum; it may take as long as a decade to accumulate enough wave observations to do large-scale studies. Fortunately, the launch will occur during the rise phase of solar cycle 24, which may present the most favorable conditions for well-defined EIT wave observations. If SDO-AIA can ultimately provide the data we require, even for a few well-observed events, we will have the opportunity to refine and potentially reconcile our currently fragmented understanding of these intriguing phenomena.

6 Conclusions

As this discussion has shown, our knowledge of EIT waves has become increasingly multi-faceted since their first discovery. While observations have improved over time, in spite of this (or perhaps because of it), our understanding has become more and more fragmented.

It is clear that no single current theory truly explains all of the physics of all EIT waves. If anything, we can only say that some models appear more correct than others, in that they offer fewer contradictions to the data. The much-favored fast-mode MHD wave theory appears to present the most problems explaining diffuse EIT waves, although it appears entirely consistent with "S-wave" and sharp X-ray wave observations. However, the results of the Linker et al. (2008) "accidental" simulation, and the Cohen et al. (2009) study suggest that some sort of MHD wave component must be present. The Wills-Davey et al. (2007) solitary wave theory goes a long way towards explaining velocity differences and magnitudes, but such a model appears difficult to simulate. The Chen et al. (2002, 2005) work, showing the EIT "waves" as a "wake" behind Moreton waves and simulating the "opening" of the magnetic field during CMEs (as first suggested by Delannée and Aulanier 1999), is also promising, but many aspects are, at present, unfalsifiable. The Attrill et al. (2007a) model of successive reconnection is able to self-consistently explain the close connection of the diffuse bright front to the CME flanks, the associated secondary dimmings, and the rotational aspects. However, no one explanation appears to be a "magic bullet."

The lack of a single coherent theory suggests that EIT waves are much more complicated than first imagined. Rather, it is likely that multiple physical processes are required to produce these coronal "waves," a premise already acknowledged by myriad studies (e.g. Thompson et al. 2000b; Biesecker et al. 2002; Chen et al. 2002; Zhukov and Auchère 2004; Cohen et al. 2009). In the end, developing a truly complete physical picture may depend less on the advocacy of any one model, and more on the success of full-faith, open-minded collaboration.

References

A. Asai, H. Hara, T. Watanabe, S. Imada, T. Sakao, N. Narukage, J.L. Culhane, G.A. Doschek, Astrophys. J. **685**, 622 (2008)

M.J. Aschwanden, L. Fletcher, C.J. Schrijver, D. Alexander, Astrophys. J. **520**, 880 (1999)

M.J. Aschwanden, N. Nitta, Astrophys. J. **535**, L59 (2000)

G. Attrill, M.S. Nakwacki, L.K. Harra, L. van Driel-Gesztelyi, C.H. Mandrini, S. Dasso, J. Wang, Sol. Phys. **238**, 117 (2006)

G.D.R. Attrill, L.K. Harra, L. van Driel-Gesztelyi, P. Démoulin, Astrophys. J. **656**, L101 (2007a)

G.D.R. Attrill, L.K. Harra, L. van Driel-Gesztelyi, P. Démoulin, J.-P. Wülser, Astron. Nachr. **328**, 760 (2007b)

G.D.R. Attrill, L. van Driel-Gesztelyi, P. Démoulin, A.N. Zhukov, K. Steed, L.K. Harra, C.H. Mandrini, J. Linker, Sol. Phys. **252**, 349 (2008)

G.D.R. Attrill, Ph.D. thesis, University College London (2008)

G.D.R. Attrill, A. Engell, M.J. Wills-Davey, P. Grigis, P. Testa, Astrophys. J. **704**, 1296 (2009)

K.S. Balasubramaniam, A.A. Pevtsov, D.F. Neidig, E.W. Cliver, B.J. Thompson, C.A. Young, S.F. Martin, A. Kiplinger, Astrophys. J. **630**, 1160 (2005)

K.S. Balasubramaniam, A.A. Pevtsov, D.F. Neidig, Astrophys. J. **658**, 1372 (2007)

I. Ballai, R. Erdélyi, ESA SP **547**, 433 (2004)

I. Ballai, R. Erdélyi, B. Pintér, Astrophys. J. **633**, L145 (2005)

U. Becker, Z. Astrophys. **44**, 243 (1958)

D.A. Biesecker, D.C. Myers, B.J. Thompson, D.M. Hammer, A. Vourlidas, Astrophys. J. **569**, 1009 (2002)

P.F. Chen, Astrophys. J. **641**, L153 (2006)

P.F. Chen, Astrophys. J. **698**, L112 (2009)

P.F. Chen, S.T. Wu, K. Shibata, C. Fang, Astrophys. J. **572**, L99 (2002)

P.F. Chen, C. Fang, K. Shibata, Astrophys. J. **622**, 1202 (2005)

E.W. Cliver, D.F. Webb, R.A. Howard, Sol. Phys. **187**, 89 (1999)

E.W. Cliver, M. Laurena, M. Storini, B.J. Thompson, Astrophys. J. **631**, 604 (2005)

O. Cohen, G.D.R. Attrill, W.B. Manchester IV, M.J. Wills-Davey, Astrophys. J. **705**, 587 (2009)

N.U. Crooker, D.F. Webb, J. Geophys. Res. **111**, A08108 (2006)

J.-P. Delaboudinière, G.E. Artzner, J. Brunaud, A.H. Gabriel, J.-F. Hochedez, F. Miller, X.Y. Song, B. Au, K.P. Dere, R.A. Howard, R. Kreplin, D.J. Michels, J.D. Moses, J.M. Defise, C. Jamar, P. Rochus, J.P. Chauvineau, J.P. Marioge, R.C. Catura, J.R. Lemen, L. Shing, R.A. Stern, J.B. Gurman, W.M. Neupert, A. Maucherat, F. Clette, P. Cugnon, E.L. van Dessel, Sol. Phys. **162**, 291 (1995)

C. Delannée, Astrophys. J. **545**, 512 (2000)

C. Delannée, Astron. Astrophys. **495**, 571 (2009)

C. Delannée, G. Aulanier, Sol. Phys. **190**, 107 (1999)

C. Delannée, J.F. Hochedez, G. Aulanier, Astron. Astrophys. **465**, 603 (2007)

C. Delannée, T. Török, G. Aulanier, J.F. Hochedez, Sol. Phys. **247**, 123 (2008)

K.P. Dere, G.E. Brueckner, R.A. Howard, M.J. Koomen, C.M. Korendyke, R.W. Kreplin, D.J. Michels, J.D. Moses, N.E. Moulton, D.G. Socker, O.C.St. Cyr, J.P. Delaboudiniére, G.E. Artzner, J. Brunaud, A.H. Gabriel, J.F. Hochedez, F. Miller, X.Y. Song, J.P. Chauvineau, J.P. Marioge, J.M. Defise, C. Jamar, P. Rochus, R.C. Catura, J.R. Lemen, J.B. Gurman, W. Neupert, F. Clette, P. Cugnon, E.L. van Dessel, P.L. Lamy, A. Llebaria, R. Schwenn, G.M. Simnett, Sol. Phys. **175**, 601 (1997)

H.W. Dodson, E.R. Hedeman, Sol. Phys. **4**, 229 (1968)

S. Eto, H. Isobe, N. Narukage, A. Asai, T. Morimoto, B. Thompson, S. Yashiro, T. Wang, R. Kitai, H. Kurokawa, K. Shibata, Proc. Astron. Soc. Jpn. **54**, 481 (2002)

G.A. Gary, Sol. Phys. **203**, 71 (2001)

H.R. Gilbert, T.E. Holzer, Astrophys. J. **610**, 572 (2004)

H.R. Gilbert, T.E. Holzer, B.J. Thompson, J.T. Burkepile, Astrophys. J. **607**, 540 (2004)

H.R. Gilbert, A.G. Daou, D. Young, D. Tripathi, D. Alexander, Astrophys. J. **685**, 629 (2008)

L. Golub, E. DeLuca, G. Austin, J. Bookbinder, D. Caldwell, P. Cheimets, J. Cirtain, M. Cosmo, P. Reid, A. Sette, M. Weber, T. Sakao, R. Kano, K. Shibasaki, H. Hara, S. Tsuneta, K. Kumagai, T. Tamura, M. Shimojo, J. McCracken, J. Carpenter, H. Haight, R. Siler, E. Wright, J. Tucker, H. Rutledge, M. Barbera, G. Peres, S. Varisco, Sol. Phys. **243**, 63 (2007)

N. Gopalswamy, M.L. Kaiser, Adv. Space Res. **29**, 307 (2002)

N. Gopalswamy, B.J. Thompson, J. Atmos. Sol.-Terr. Phys. **62**, 1457 (2000)

N. Gopalswamy, M.L. Kaiser, J. Sato, M. Pick, in *High Energy Solar Physics Workshop - Anticipating Hess*, ed. by R. Ramaty, N. Mandzhavidze. Astronomical Society of the Pacific Conference Series, vol. 206 (2000), p. 351

N. Gopalswamy, S. Yashiro, M. Temmer, J. Davila, W.T. Thompson, S. Jones, R.T.J. McAteer, J.-P. Wuelser, S. Freeland, R.A. Howard, Astrophys. J. **691**, L123 (2009)

V.V. Grechnev, I.M. Chertok, V.A. Slemzin, S.V. Kuzin, A.P. Ignat'ev, A.A. Pevtsov, I.A. Zhitnik, J.-P. Delaboudiniére, F. Auchère, J. Geophys. Res. **110**, A09S07 (2005)

B.N. Handy, L.W. Acton, C.C. Kankelborg, C.J. Wolfson, D.J. Atkin, M.E. Bruner, R. Caravalho, R.C. Catura, R. Chevalier, D.W. Duncan, C.G. Edwards, C.N. Feinstein, F.M. Friedlaender, C.H. Hoffman, N.E. Hurlburt, B.K. Jurcevich, N.L. Katz, G.A. Kelly, J.R. Lemen, M. Levay, R.W. Lindgren, D. Mathur, R.W. Nightingale, T.P. Pope, R.A. Rehse, C.J. Schrijver, R.A. Shine, L. Shing, K.T. Strong, T.D. Tarbell, A.M. Title, D.D. Torgerson, L. Golub, J.A. Bookbinder, D. Caldwell, P.N. Cheimets, W.N. Davis, E.E. Deluca, R.A. McMullen, H.P. Warren, D. Amato, R. Fisher, H. Maldonado, C. Parkinson, Sol. Phys. **187**, 229 (1999)

L.K. Harra, A.C. Sterling, Astrophys. J. **561**, L215 (2001)

L.K. Harra, A.C. Sterling, Astrophys. J. **587**, 429 (2003)

L.K. Harra, H. Hara, S. Imada, P.R. Young, D.R. Williams, A.C. Sterling, C. Korendyke, G.D.R. Attrill, Publ. Astron. Soc. Jpn. **59**, S801 (2007)

R.A. Harrison, M. Lyons, Astron. Astrophys. **358**, 1097 (2000)

M. Hata, Master's Dissertation, Science University of Tokyo (2001)

H.S. Hudson, D.F. Webb, AGU Monograph (1997)

H.S. Hudson, J.I. Khan, J.R. Lemen, N.V. Nitta, Y. Uchida, Sol. Phys. **212**, 121 (2003)

S. Imada, H. Hara, T. Watanabe, A. Asai, S. Kamio, K. Matsuzaki, L.K. Harra, J.T. Mariska, Publ. Astron. Soc. Jpn. **59**, S793 (2007)

M.L. Kaiser, Adv. Space Res. **36**, 1483 (2005)

M.L. Kaiser, T.A. Kucera, J.M. Davila, O.C. St. Cyr, M. Guhathakurta, E. Christian, Space Sci. Rev. **136**, 5 (2008)

J.L. Khan, H. Aurass, Astron. Astrophys. **383**, 1018 (2002)

J.L. Khan, H.S. Hudson, Geophys. Res. Lett. **27**, 1083 (2000)

I.W. Kienreich, M. Temmer, A.M. Veronig, Astron. Astrophys. **703**, L118 (2009)

A. Klassen, H. Aurass, G. Mann, B.J. Thompson, Astron. Astrophys. Suppl. Ser. **141**, 357 (2000)

V. Krasnoselskikh, O. Podladchikova, AGU Fall Meet. Abstr. A1047 (2007)

J.R. Lemen, D.W. Duncan, C.G. Edwards, F.M. Friedlaender, B.K. Jurcevich, M.D. Morrison, L.A. Springer, R.A. Stern, J.-P. Wuelser, M.E. Bruner, R.C. Catura, Proc. SPIE **5171**, 65 (2004)

J. Linker, Z. Mikic, P. Riley, R. Lionello, V. Titov, 37th COSPAR Abstr. D22-0008-08 (2008)

D.M. Long, P.T. Gallagher, R.T.J. McAteer, D.S. Bloomfield, Astrophys. J. **680**, L81 (2008)

S. Ma, M.J. Wills-Davey, J. Lin, P.F. Chen, G.D.R. Attrill, H. Chen, S. Zhao, Q. Li, L. Golub, Astrophys. J. (2009, in press)

C.H. Mandrini, S. Pohjolainen, S. Dasso, L.M. Green, P. Démoulin, L. van Driel-Gesztelyi, C. Copperwheat, C. Foley, Astron. Astrophys. **434**, 725 (2005)

C.H. Mandrini, M.S. Nakwacki, G. Attrill, L. van Driel-Gesztelyi, P. Démoulin, S. Dasso, H. Elliott, Sol. Phys. **244**, 25 (2007)

G. Mann, A. Klassen, C. Estel, B.J. Thompson, ESA SP **446**, 447 (1999)

S.W. McIntosh, R.J. Leamon, A.R. Davey, M.J. Wills-Davey, Astrophys. J. **660**, 1653 (2007)

J.A. McLaughlin, L. Ofman, Astrophys. J. **682**, 1338 (2008)

F. Meyer, in *Structure and Development of Solar Active Regions*. IAU, 485 (1968)

R.L. Moore, A.C. Sterling, S.T. Suess, Astrophys. J. **668**, 1221 (2007)

G.E. Moreton, Astron. J. **65**, 494 (1960)

G.E. Moreton, H.E. Ramsey, Publ. Astron. Soc. Pac. **72**, 357 (1960)

D. Moses, F. Clette, J.-P. Delaboudiniére, G.E. Artzner, M. Bougnet, J. Brunaud, C. Carabetian, A.H. Gabriel, J.F. Hochedez, F. Millier, X.Y. Song, B. Au, K.P. Dere, R.A. Howard, R. Kreplin, D.J. Michels, J.M. Defise, C. Jamar, P. Rochus, J.P. Chauvineau, J.P. Marioge, R.C. Catura, J.R. Lemen, L. Shing, R.A. Stern, J.B. Gurman, W.M. Neupert, J. Newmark, B. Thompson, A. Maucherat, F. Portier-Fozzani, D. Berghmans, P. Cugnon, E.L. van Dessel, J.R. Gabryl, Sol. Phys. **175**, 571 (1997)

N. Narukage, H.S. Hudson, T. Morimoto, S. Akiyama, R. Kitai, H. Kurokawa, K. Shibata, Astrophys. J. **572**, L109 (2002)

N. Narukage, T. Morimoto, M. Kadota, R. Kitai, H. Kurokawa, K. Shibata, Publ. Astron. Soc. Jpn. **56**, L5 (2004)

N. Narukage, T. Ishii, S. Nagata, S. UeNo, R. Kitai, H. Kurokawa, M. Akioka, K. Shibata, Astrophys. J. **684**, L45 (2008)

D. Neidig, AAS Meet. **204**, #47.10 (2004)

G.J. Nelson, D.B. Melrose, Sol. Radiophys. 333 (1985)

W.M. Neupert, Astrophys. J. **344**, 504 (1989)

A.H. Nye, J.H. Thomas, Astrophys. J. **204**, 573 (1976)

L. Ofman, Space Sci. Rev. **120**, 67 (2005)

L. Ofman, Astrophys. J. **655**, 1134 (2007)

L. Ofman, B.J. Thompson, Astrophys. J. **574**, 440 (2002)

T.J. Okamoto, H. Nakai, A. Keiyama, N. Narukage, S. UeNo, R. Kitai, H. Kurokawa, K. Shibata, Astrophys. J. **608**, 1124 (2004)

S. Patsourakos, A. Vourlidas, Astrophys. J. **700**, L182 (2009)

S. Patsourakos, A. Vourlidas, Y.M. Wang, G. Stenborg, A. Thernisien, Sol. Phys. **259**, 49 (2009)

S.P. Plunkett, B.J. Thompson, R.A. Howard, D.J. Michels, O.C.St. Cyr, S.J. Tappin, R. Schwenn, P.L. Lamy, Geophys. Res. Lett. **25**, 2477 (1998)

O. Podladchikova, D. Berghmans, Sol. Phys. **228**, 265 (2005)

S. Pohjolainen, D. Maia, M. Pick, N. Vilmer, J.I. Khan, W. Otruba, A. Warmuth, A. Benz, C. Alissandrakis, B.J. Thompson, Astrophys. J. **556**, 421 (2001)

D.M. Rust, Space Sci. Rev. **34**, 21 (1983)

D.M. Rust, E. Hildner, Sol. Phys. **48**, 381–387 (1976)

K. Schwer, R.B. Lilly, B.J. Thompson, D.A. Brewer, AGU Abstr. SH21C-01 (2002)

S.F. Smith, K.L. Harvey, Astrophys. Space Sci. Lib. **27**, 156 (1971)

A.C. Sterling, H.S. Hudson, Astrophys. J. **491**, L55 (1997)

M. Temmer, A. Veronig, B. Vrsnak, J. Thalmann, A. Hanslmeier, ESA SP 600 (2005)

J. Terradas, L. Ofman, Astrophys. J. **610**, 523 (2004)

B.J. Thompson, D.C. Myers, Astrophys. J. Suppl. Ser. **183**, 225 (2009)

B.J. Thompson, S.P. Plunkett, J.B. Gurman, J.S. Newmark, O.C.St. Cyr, D.J. Michels, Geophys. Res. Lett. **25**, 2465 (1998)

B.J. Thompson, J.B. Gurman, W.M. Neupert, J.S. Newmark, J.-P. Delaboudinière, O.C.St. Cyr, S. Stezelberger, K.P. Dere, R.A. Howard, D.J. Michels, Astrophys. J. **517**, L151 (1999)

B.J. Thompson, E.W. Cliver, N. Nitta, C. Delannée, J.-P. Delaboudinière, Geophys. Res. Lett. **27**, 1431 (2000a)

B.J. Thompson, B. Reynolds, H. Aurass, N. Gopalswamy, J.B. Gurman, H.S. Hudson, S.F. Martin, O.C.St. Cyr, Sol. Phys. **193**, 161 (2000b)

A.M. Title, the AIA team, Bull. Am. Astron. Soc. **38**, 261 (2006)

T. Török, B. Kliem, Astron. Astrophys. **406**, 1043 (2003)

S. Tsuneta, L. Acton, M. Bruner, J. Lemen, W. Brown, R. Caravalho, R. Catura, S. Freeland, B. Jurcevich, J. Owens, Sol. Phys. **136**, 37 (1991)

Y. Uchida, Sol. Phys. **4**, 30 (1968)

Y. Uchida, Sol. Phys. **39**, 431 (1974)

Y. Uchida, A. Martin, G. Newkirk, Sol. Phys. **28**, 495 (1973)

L. van Driel-Gesztelyi, G.D.R. Attrill, P. Démoulin, C.H. Mandrini, L.K. Harra, Ann. Geophys. **26**, 3077 (2008)

A.M. Veronig, M. Temmer, B. Vrsnak, J.K. Thalmann, Astrophys. J. **647**, 1466 (2006)

A.M. Veronig, M. Temmer, B. Vrsnak, Astrophys. J. **681**, L113 (2008)

B. Vrsnak, EOS Trans. **86**, 112 (2005)

B. Vrsnak, A. Warmuth, R. Brajsa, A. Hanslmeier, Astron. Astrophys. **394**, 299 (2002)

B. Vrsnak, E.W. Cliver, Sol. Phys. **253**, 215 (2008)

B. Vrsnak, J. Magdalenic, M. Temmer, A. Veronig, A. Warmuth, G. Mann, H. Aurass, W. Otruba, Astrophys. J. **625**, L67 (2005)

H. Wang, C. Shen, J. Lin, Astrophys. J. **700**, 1716 (2009)

Y.M. Wang, Astrophys. J. **543**, L89 (2000)

T. Wang, Y. Yan, J. Wang, H. Kurokawa, K. Shibata, Astrophys. J. **572**, 580 (2002)

A. Warmuth, Lect. Not. Phys. **725**, 107 (2007)

A. Warmuth, G. Mann, Astron. Astrophys. **435**, 1123 (2005)

A. Warmuth, B. Vrsnak, H. Aurass, A. Hanslmeier, Astrophys. J. **560**, L105 (2001)

A. Warmuth, B. Vrsnak, J. Magdalenic, A. Hanslmeier, W. Otruba, Astron. Astrophys. **418**, 1101 (2004a)

A. Warmuth, B. Vrsnak, J. Magdalenic, A. Hanslmeier, W. Otruba, Astron. Astrophys. **418**, 1117 (2004b)

A. Warmuth, G. Mann, H. Aurass, Astrophys. J. **626**, L121 (2005)

D.F. Webb, R.P. Lepping, L.F. Burlaga, C.E. DeForest, D.E. Larson, S.F. Martin, S.P. Plunkett, D.M. Rust, J. Geophys. Res. **105**, 27251 (2000)

Y. Wen, J. Wang, D.J.F. Maia, Y. Zhang, H. Zhao, G. Zhou, Sol. Phys. **239**, 257 (2006)

S.M. White, B.J. Thompson, Astrophys. J. **620**, L63 (2005)

J.P. Wild, L.L. McCready, Austral. J. Sci. Res., A **3**, 387 (1950)

M.J. Wills-Davey, Ph.D. thesis, Montana State University (2003)

M.J. Wills-Davey, Astrophys. J. **645**, 757 (2006)

M.J. Wills-Davey, M. Sechler, AGU Fall Meet. #SH31A-0222 (2007)

M.J. Wills-Davey, B.J. Thompson, Sol. Phys. **190**, 467 (1999)

M.J. Wills-Davey, C.E. DeForest, J.O. Stenflo, Astrophys. J. **664**, 556 (2007)

S.T. Wu, H. Zheng, S. Wang, B.J. Thompson, S.P. Plunkett, X.P. Zhao, M. Dryer, J. Geophys. Res. **106**, 25089 (2001)

J.-P. Wuelser, J.R. Lemen, T.D. Tarbell, C.J. Wolfson, J.C. Cannon, B.A. Carpenter, D.W. Duncan, G.S. Gradwohl, S.B. Meyer, A.S. Moore, R.L. Navarro, J.D. Pearson, G.R. Rossi, L.A. Springer, R.A. Howard, J.D. Moses, J.S. Newmark, J.-P. Delaboudinière, G.E. Artzner, F. Auchère, M. Bougnet, P. Bouyries, F. Bridou, J.-Y. Clotaire, G. Colas, F. Delmotte, A. Jerome, M. Lamare, R. Mercier, M. Mullot, M.-F. Ravet, X. Song, V. Bothmer, W. Deutsch, SPIE Conf. Proc. **5171**, 111 (2004)

S. Yashiro, N. Gopalswamy, G. Michalek, O.C. St. Cyr, S.P. Plunkett, N.B. Rich, R.A. Howard, J. Geophys. Res. **109**, A07105 (2004)

I.A. Zhitnik, O.I. Bougaenko, J.-P. Delaboudinière, A.P. Ignatiev, V.V. Korneev, V.V. Krutov, S.V. Kuzin, D.V. Lisin, A.V. Mitrofanov, S.N. Oparin, V.N. Oraevsky, A.A. Pertsov, V.A. Slemzin, I.I. Sobelman, A. I Stepanov, J. Schwarz, in Solar Variability: From Core to Outer Frontiers. ESA SP **506**, 915 (2002)

A.N. Zhukov, F. Auchère, Astron. Astrophys. **427**, 705 (2004)

A.N. Zhukov, L. Rodriguez, J. de Patoul, Sol. Phys. **259**, 73 (2009)